

Artifact Analysis and Removal of Electroencephalographic (EEG) Recordings

Yi Dou

A Thesis

in

The Department

of

Concordia Institute for Information Systems Engineering

Presented in Partial Fulfillment of the Requirements

for the Degree of

Master of Applied Science (Quality System Engineering) at

Concordia University

Montréal, Québec, Canada

March 2017

© Yi Dou, 2017

CONCORDIA UNIVERSITY
School of Graduate Studies

This is to certify that the thesis prepared

By: **Yi Dou**

Entitled: **Artifact Analysis and Removal of Electroencephalographic
(EEG) Recordings**

and submitted in partial fulfillment of the requirements for the degree of

Master of Applied Science (Quality System Engineering)

complies with the regulations of this University and meets the accepted standards with respect to originality and quality.

Signed by the Final Examining Committee:

_____ Chair
Dr. Jia Yuan Yu

_____ External Examiner
Dr. Zhi Chen (BCEE)

_____ Examiner
Dr. Jia Yuan Yu

_____ Supervisor
Dr. Yong Zeng

_____ Co-supervisor
Dr. Wei-Ping Zhu (ECE)

Approved by

Rachida Dssouli, Chair
Department of Concordia Institute for Information Systems
Engineering

2017

Amir Asif, Dean
Faculty of Engineering and Computer Science

Abstract

Artifact Analysis and Removal of Electroencephalographic (EEG) Recordings

Yi Dou

Electroencephalography (EEG) technique has been widely used in continuous monitoring the brain activities in academic research and clinical applications. In cognitive neuroscience research, the electrical brain signals can be used to measure mental effort of subjects. However, the presence of artifacts is a constant problem when recording brain activities, which will obscure the underlying neural dynamics and therefore make it difficult to interpret EEG signals accurately. These unwanted signals or artifacts have different effects depending on their sources of generation. Among them, the motion of the subject is one of the major contributors to physiological artifacts that causes most of the contaminations to the underlying brain activities. It is quite challenging to correct the myogenic activity from EEG background potentials due to its wide spectral distribution overlapped with typical bands of brain waves related to cognitive activities, and the spatial distribution over the entire scalp of human. As such, this thesis focuses on the analysis and removal of motion artifacts from EEG signals.

The preliminary investigations include the movement-triggered artifact identification and the analysis of the characteristics of the motion artifact. According to the recorded video, the contaminated epochs are extracted from the original EEG signals. A set of features of the movement-triggered artifacts are proposed based on power spectral density and wavelet transform. Statistical analysis is performed to distinguish the segments that

contain motions. Two typical methods of artifact removal are then studied, and the efficiency to correct this type of artifact is validated by comparing the extracted features of non-movement segments and the contaminated segments. The result shows that the tested artifact removal methods cannot completely remove movement artifacts, which also infers the potential relation between motion and mental activities.

Acknowledgments

First and foremost, I would like to express my profound appreciation to my supervisors Dr. Yong Zeng and Dr. Wei-Ping Zhu, for their constant guidance and support throughout the course of my graduate study and research. It would not be possible to complete this thesis without their insightful advice and inspiration. It is a great fortune to have the opportunity to work with two such outstanding professors. I am impressed and motivated by their enthusiasm for the research, and I benefited greatly from their knowledge and wisdom.

I would also like to thank all my colleagues in the Design Lab. It is very fortunate to be in this friendly research environment and collaborate with all the past and present group members. Special thanks to Dr. Thanh An Nguyen, for her help and valuable advice in EEG research. I gratefully acknowledge all the friends that made my time at Concordia enjoyable.

Last but not the least, I would like to thank my beloved parents, for providing me with the continuous encouragement and unconditional love in my life. Thank you.

Contents

List of Figures	ix
List of Tables	xi
1 Introduction	1
1.1 Background and Motivation	1
1.2 Objective	4
1.3 Contribution	4
1.4 Thesis organization	5
2 Background Material	6
2.1 Electroencephalography (EEG)	6
2.1.1 Lobes of the brain	7
2.1.2 Brain waves	9
2.1.3 Event-related potentials (ERPs)	10
2.2 Artifacts	12
2.2.1 Typical artifacts	13
2.2.2 Movement-triggered artifact	16
3 Signal Collection and Experimental Setup	18
3.1 Selection of participants	18

3.2	EEG signal recording	19
3.3	Movement recording	21
3.4	Experiment procedure	22
3.5	Data pre-processing	24
4	Movement-triggered Artifact Analysis	26
4.1	EEG data segmentation	27
4.2	Feature extraction in artifact analysis	31
4.2.1	Power spectral analysis	32
4.2.2	Wavelet analysis	36
4.3	Experimental results	40
4.3.1	Results using relative Beta2 power	40
4.3.2	Results using wavelet entropy	46
5	Artifact Removal	49
5.1	Canonical correlation analysis (CCA)	50
5.2	Independent component analysis (ICA)	54
5.3	Experimental results	57
5.3.1	CCA	57
5.3.2	ICA	63
5.4	Discussion	68
6	Conclusion and Future Work	69
6.1	Conclusion	69
6.2	Future Work	71
	Bibliography	73

List of Figures

Figure 2.1	EEG signals from an adult with twenty-one electrodes at various sites on the brain scalp.	7
Figure 2.2	Brain lobes.	8
Figure 3.1	64-Ch standard electrode layout.	20
Figure 3.2	Video recording from the experiment.	22
Figure 3.3	The location of three web cameras.	23
Figure 3.4	Four stages of the experiment.	23
Figure 4.1	The overview of movement-triggered artifact analysis.	27
Figure 4.2	Segmentation process and relation between video and EEG.	28
Figure 4.3	Three types of segments in the time domain.	31
Figure 4.4	Power spectral density (PSD) of one subject in a specific movement.	35
Figure 4.5	EEG signal decomposition based on DWT.	38
Figure 4.6	A graphical user interface (GUI) for data analysis.	41
Figure 4.7	An example of PSD in graphical user interface (GUI).	42
Figure 4.8	Comparison of means (a) and variances (b) of relative Beta2 power for each channel.	43
Figure 4.9	Statistical analysis of relative Beta2 power for all channels.	44
Figure 4.10	Statistical analysis of spectral edge frequency (SEF) for all channels in test period.	45
Figure 4.11	Grand mean of relative Beta2 power in four types of movements.	47

Figure 4.12 Comparison of means (a) and variances (b) of wavelet entropy for three types of segments.	47
Figure 4.13 Statistical analysis of relative wavelet entropy (RWE) for all channels.	48
Figure 5.1 General framework of signal combination.	50
Figure 5.2 Experimental procedure of movement-triggered artifact removal. . .	51
Figure 5.3 Comparison of means (a) and variances (b) of relative Beta2 power for each channel after applying CCA.	58
Figure 5.4 Statistical analysis of relative Beta2 power for all channels after applying CCA.	59
Figure 5.5 Statistical analysis of spectral edge frequency (SEF) for all channels in reconstructed period after applying CCA.	60
Figure 5.6 Comparison of means (a) and variances (b) of wavelet entropy for each channel after applying CCA.	61
Figure 5.7 Statistical analysis of relative wavelet entropy (RWE) for all channels after applying CCA.	62
Figure 5.8 Comparison of means (a) and variances (b) of relative Beta2 power for each channel after applying ICA.	63
Figure 5.9 Statistical analysis of relative Beta2 power for all channels after applying ICA.	64
Figure 5.10 Statistical analysis of spectral edge frequency (SEF) for all channels in context period (a) and test period (b) after applying ICA.	65
Figure 5.11 Comparison of means (a) and variances (b) of wavelet entropy for each channel after applying ICA.	66
Figure 5.12 Statistical analysis of relative wavelet entropy (RWE) for all channels after applying ICA.	67

List of Tables

Table 3.1	Number of segments for each subject.	24
Table 4.1	Time table of physical movements for segmentation	30
Table 4.2	P value for colored channels in test period (Beta2).	45
Table 4.3	P-value for colored channels in test period (SEF).	46
Table 4.4	P value for colored channels in test period (RWE).	48

Chapter 1

Introduction

1.1 Background and Motivation

Electroencephalography is a non-invasive measurement of brain activity, which could be used to record the electrical activity of brain from the scalp related to cortical activity. Early in 1920s, Hans Berger first measured the brain activity on human scalp, and defined the word electroencephalogram for describing brain electric potentials. Also, it is conjectured that periodic fluctuation of EEG might be related with general cognitive states of subjects, including arousal and consciousness. Over the past several years, researchers have actively studied EEG to understand the cognitive process.

Recently, a variety of imaging techniques have been applied for studying brain functions of human, such as magnetic resonance imaging (MRI), positron emission tomography (PET) and single photon emission computed tomography (SPECT). These measurements can provide good spatial resolution of two or three dimensional images. However, EEG is still a powerful and frequently-used tool in modern medicine field and academia to measure brain activity with its own advantages. Above all, EEG has a relative high temporal resolution for data processing compared with above-mentioned imaging techniques, which

is essential for real-time monitoring. Besides that, the total cost of EEG recording instrumentation is extremely lower than others, with the use of electrodes, conductive media and computer software for signal storage and analysis (Teplan, 2002).

To trace the bioelectric potentials in brain, electrodes are used to place directly on human skin. When the nerve or muscle cells are activated, ionic potentials are produced. The effect of electrodes is to convert these ionic potentials into electrical potentials which can be measured. Since EEG is obtained directly from the scalp surface, this procedure can be applied repeatedly to normal adults, children and patients nearly without risk and limitation.

EEG signal has a wide range of applications in modern medicine. Since EEG contains a lot of information reflecting the state of body health and different physiological states of the brain, it is one of the most commonly-used tools for monitoring the neurological disorders, such as epileptic seizures (McGrogan et al., 1999). In order to detect the time when the epileptic activity occurs, long-term monitoring is always employed. Apart from that, other applications include the evaluation of brain activity during human sleep and severity of sleep disorders (Carskadon & Rechtschaffen, 2000) (Berka et al., 2005), the assessment of mental workload (Gevins et al., 1998) (Gevins & Smith, 2003) (Berka et al., 2007) and brain-computer interfaces (BCI) (Wolpaw & McFarland, 2004).

No matter which fields the EEG signals are applied to, it is critical to ensure the high quality of the recorded signals. Normally, the neural EEG signals are in the range of micro volts, and it can be masked by undesired potentials mostly generated from non-cerebral origin, which are called artifacts. In academic studies and clinical applications, the presence of artifact is a constant problem during the recording of brain activity. These unwanted signals always have different forms of effects depending on the sources of the artifacts. Among all types of artifacts, electrooculography (EOG) and electromyography (EMG) artifacts are two major contributors of physiological artifacts that cause most of contaminations to the

underlying brain activity.

As reviewed in (Fatourechi, Bashashati, Ward, & Birch, 2007), the consideration of EMG and/or EOG artifacts are not reported in most BCI papers published until 2006, and the number of studies that did not report EMG artifacts is higher than that of EOG.

With the help of a series of electrodes settled close to the eyes as reference channels, the electrooculogram (EOG) can be recorded for dealing with eye-movement artifacts. The most common technique for ocular artifact removal is based on linear combination and regression (Croft & Barry, 2000). Furthermore, it is argued that the error in the subtraction phase is small relative to the main EOG correction (Croft & Barry, 2002).

However, since there is no reference channel for EMG artifact, it is particularly challenging to correct muscle artifact, which has high amplitude, broad frequency distribution and variable topographical distribution, as investigated in (Goncharova, McFarland, Vaughan, & Wolpaw, 2003). In clinical practice, the entire affected segments of data would be rejected in most circumstances, while it will definitely lead to a considerable information loss.

There exists a variety of methods for artifact separation and removal. By using simple filtering techniques, such as band pass filters, the separation could be accomplished in frequency domain. However, since the frequency of artifact and the desired signal are always overlapped in actual situations, alternative techniques should be applied.

Methods of blind source separation (BSS) are currently utilized in signal processing for removing artifact. Based on the assumption that the neural activity and artefactual signal are not systematically co-activated, the separation is performed after the transformation of the recorded EEG signals into a set of source components. There are several algorithms to perform BSS, including canonical correlation analysis (CCA) (Clercq, Vergult, Vanrumste, Paesschen, & Huffel, 2006) and independent component analysis (ICA) (Jung et al., 2000), which are employed in this thesis for artifact removal.

1.2 Objective

The objective of this thesis is two-fold. The first objective is to analyze the artifacts generated from the voluntary motions of subjects during a cognitive task, and investigate the characteristics of artefactual segments through feature extraction, which is performed by the Fast Fourier Transform (FFT) method in the frequency domain and the Wavelet Transform (WT) in the time-frequency domain. The second objective is to remove this type of artifacts in EEG recordings by two existing artifact removal techniques, and validate their performances.

1.3 Contribution

The contributions of this thesis are described below.

- A comprehensive literature review of the artifacts in EEG signals and the state of the art in artifact removal techniques are presented.
- A guideline is provided to extract the EEG segments contaminated by movement-triggered artifacts based on the video recording of the experiments of subjects.
- A graphic user interface is developed to extract the features for movement-related signal analysis, and distinguish the statistical differences when movement occurs in scalp map.
- Two typical techniques of artifact removal are attempted, and the performances are evaluated according to feature extraction results.

1.4 Thesis organization

The rest of this thesis consists of the following five chapters. The content of each chapter is described below:

Chapter 2 introduces the basic background of the physiological signal in human brain, which is called electroencephalography (EEG). The relevant signal waves and artifacts are also described with the commonly used classification.

Chapter 3 provides a brief introduction of the cognitive experiment in 2015, which measures the physiological signals concerning mental effort during design activities. With the help of video recording, all the useful information was collected for movement-triggered artifact analysis.

Chapter 4 analyzes the movement-triggered EEG signals generated from the cognitive experiment, as presented in segmentation section and feature extraction section. For manual screening and marking of artifacts, a set of criteria are proposed, which will be used to extract the affected segments from the EEG recording. At the same time, the comparison of different features is also presented.

Chapter 5 focuses on the study of various methods for artifact removal. Among these techniques, two of them are described in detail, namely canonical correlation analysis (CCA) and independent component analysis (ICA). Furthermore, the selection of artifact components is studied in this chapter. A comparison of results is also presented.

Chapter 6 summarizes the research results of this thesis and suggests some topics for future work.

Chapter 2

Background Material

2.1 Electroencephalography (EEG)

In cognitive neuroscience research, it is generally known that there exists a modular organization in the brain. These discrete units of modules are functionally constructed, and they interact to the generation of mental activities. The aim of this research is to investigate the neural basis of cognition and figure out how the different areas of brain support cognitive functions (Gazzaniga, 1989). To this end, the anterior cingulate cortex (ACC) has been discussed, and it is suggested that ACC has a relationship with mental effort by using event-related potentials (Mulert, Menzinger, Leicht, Pogarell, & Hegerl, 2005). Apart from that, the dynamic of ACC activity can be investigated by functional imaging techniques.

Design can usually be considered as a high level cognitive ability. The design activity can be studied by measuring physiological signals as well, such as functional magnetic resonance imaging (fMRI) (Alexiou, Zamenopoulos, Johnson, & Gilbert, 2009) and electroencephalography (EEG). During cognitive processes, electrical brain signals can be applied to identify mental design activities (Nguyen & Zeng, 2012) and measure mental effort of subjects (Nguyen & Zeng, 2014). Various EEG features are introduced to reflect mental

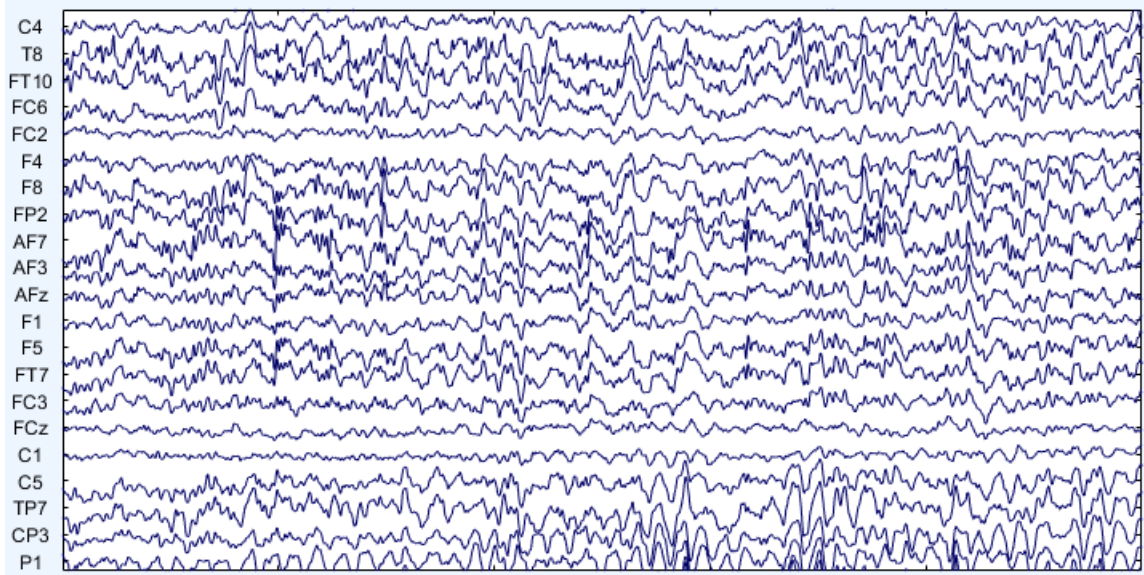


Figure 2.1: EEG signals from an adult with twenty-one electrodes at various sites on the brain scalp.

effort in many studies. For example, in (Howells, Stein, & Russell, 2010), perceived mental effort is correlated with Beta band power.

The ultimate goal in our research is to explore the cognitive effort during design process by using EEG signals. Figure 2.1 shows the EEG waveforms commonly observed in the experiment. In order to make sure the EEG recording conveys the correct and valuable information in cognitive research, the investigation of signal quality is quite important. The presence of artifact may produce unwanted changes during monitoring and thus affect the signals of interest, especially for long term recordings.

2.1.1 Lobes of the brain

The largest portion of the human brain is the telencephalon, which can be divided into lobes. Considering the anatomical classification and different brain functions, the cerebrum consists of six lobes of brain in Terminologia Anatomica (Ribas, 2010).

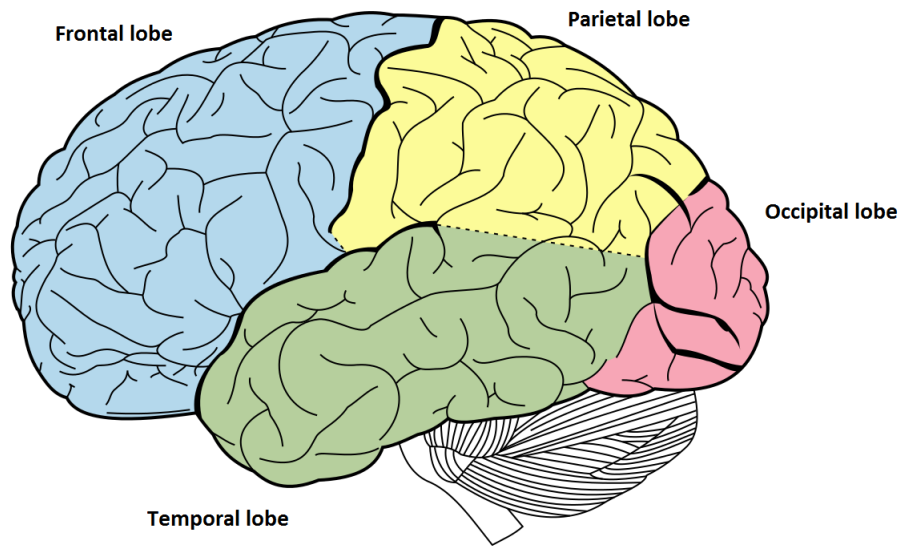


Figure 2.2: Brain lobes.

There are four major lobes of the cerebral cortex in human brain, frontal, parietal, temporal and occipital lobe, as shown in Figure 2.2. The locations and functions are introduced as follows:

- Frontal lobe:

The space at the front of cerebral hemisphere is called frontal lobe, which usually contains dopamine-delicate neurons, and it is involved in attention, short-time memory tasks, planning and motivation.

- Parietal lobe:

The parietal lobe is located above the occipital lobe and behind the frontal lobe. The sensory information in different modalities is collected in this area, including spatial sense and sensory input for the skin. In addition, several regions in parietal lobe play an important role in language processing.

- Temporal lobe:

The region beneath the lateral fissure on two sides of cerebral hemispheres is called temporal lobe. It is associated with visual memories, language comprehension, and emotion association.

- Occipital lobe:

Since the occipital lobe contains most of the anatomical region of visual cortex, it is considered as the visual processing center of the brain. Extrastriate regions are related to different tasks, such as visuospatial processing, motion perception and color differentiation.

2.1.2 Brain waves

In order to provide a constant recording of electrical activity of the brain for brain researchers and clinical experts, two basic parameters: amplitude and frequency are used to describe EEG. Some of the EEG patterns are quite reliable for visual inspection. In general, there are five typical brain waves classified by different frequency ranges, and these rhythms are identified by Greek letters respectively as δ (delta), θ (theta), α (alpha), β (beta) and γ (gamma). Berger introduced the alpha and beta waves in 1929. Jasper and Andrews named the gamma wave in 1938. Delta and theta rhythms were introduced by [Walter \(1953\)](#).

Delta activity refers to EEG activity in the 0.5-4 Hz. It is mostly associated with EEG-synchronized sleep in humans. In the first years of life for human infants, the predominant frequency is also delta rhythm.

Theta activity can be seen with a low frequency range of 4-8 Hz. [Schacter \(1977\)](#) indicates that theta activity is related to two psychological events. The first one is a low level of alertness in hypnagogic and sleep deprivation states. On the other hand, in problem-solving and perceptual processing, theta is associated with active and efficient processing.

Alpha activity occurs over the posterior regions of the head, and in most of individuals

when they are awake and relaxed. The alpha rhythm consists of relative high voltage, which is normally less than 50 μ V, over the occipital areas within the range of 8 to 13 Hz. The presence is related to physical relaxation with eye closed and relative mental inactivity (Niedermeyer & da Silva, 2005).

The usual waking rhythm of the brain is beta wave, which is related to active thinking, active attention and solving concrete problems in normal adults. Normally, beta wave has low-voltage variations with the range of 13 to 30 Hz.

A higher frequency range from 30 to 70 Hz or more with lower voltage variations is gamma rhythm.

2.1.3 Event-related potentials (ERPs)

Event-related responses are evoked responses regardless of the nature of the stimulus. To a specific event, such as visual, auditory stimulus and motor action, there exist some consistent brain responses as the underlying assumption. ERPs are time-locked, and could be divided into endogenous and exogenous ERPs. The former ERPs refer to the physical nature of the stimulus, and the second ERPs are controlled by the individuals perception or interpretation of the event. Unlike the spontaneous EEG, ERP has smaller voltage and requires averaging procedures across trials to enhance the response.

Normally, the first step of ERP procedure is to time lock the EEG signals to each event of interest, and define them as epochs. Each epoch has a certain duration. After repeating the stimulus several times, these epochs are averaged across trials for each experimental condition. The averaged event-related response can be obtained at both individual and group levels.

For further analysis, we define the ERP components as waveform elements that emerge from the baseline of the recording. The nomenclatures of ERP component can reflect the polarity (positive or negative deflection), timing and scalp distribution. However, it is quite

difficult to get ERP component, because the voltage deflections of the resulting ERP reflect the sum of several relatively independent underlying to latent components, and it is difficult to isolate the latent components. Thus, a set of rules were proposed by [Luck \(2005\)](#) to avoid misinterpreting the relationship between the observable peaks and the underlying components.

Event-related potential (ERP) technique has a better performance for studying perception and attention than other techniques, such as fMRI and PET. Since ERPs have a precise temporal resolution based on the sample rate, the brain activity can be measured on a scale of tens of milliseconds, as well as many aspects of attention and perception in operation ([Woodman, 2010](#)).

Early in 1951, Bates recorded cerebral potentials associated with voluntary muscular movements by superimposing EEG tracing. With the EMG signals recorded by surface electrodes to obtain the onset of motor contraction, he found a small potential change after the onset of electromyogram. Later, by repeating movements and averaging EEG segments off-line, [Kornhuber and Deecke \(1965\)](#) found the Bereitschaftspotential (BP) or readiness potential (RP) preceding the EMG onset. Two more components were then identified as pre-motion positivity and motor potential, just before the onset of EMG in ([Deecke, Scheid, & Kornhuber, 1969](#)). Since then, the interest for movement-related cortical potentials (MRCP) has widely increased.

Pre-movement activity refers to the time of movement preparation when the subject is going to perform afterwards, but no muscle movement is detectable. Study shows that BP usually starts around 2 s before the movement onset in ([Shibasaki & Hallett, 2006](#)). The changes before movements and brain status could provide useful information in practical applications. For example, in brain computer interfaces (BCIs), BP can predict the intention and direction of the upcoming movement, and even determine the future moving limb, as reviewed in ([Ahmadian, Cagnoni, & Ascari, 2013](#)).

However, movement-triggered artifact analysis is not a typical ERP problem in this thesis, since the movements generated by the subjects is not repeatable. In addition, the magnitude of muscle movement artifact is greater than the ERP.

2.2 Artifacts

According to the International Federation of Clinical Neurophysiology (IFCN), artifact is defined as any potential difference due to an extra-cerebral source, recorded in EEG tracing. Contamination of the EEG signals by artifact is a well-recognized problem for clinical and experimental electroencephalography. Since EEG activity would be obscured by artifact, which will lead to misinterpretation and false conclusions ([Klass, 1995](#)).

It is always a challenge to deal with artifact for the academic studies, both excellent training and considerable experience are required. The first thing is to recognize the existence of artifacts, and then, identify the type and determine the source. After that, eliminate the artifact if possible. However, artifacts may have similar parameters in rhythmicity, frequency and recurrence compared to the recorded potentials of cerebral origin. So it would become quite difficult to figure out the distinction between artefactual and cerebral electrical activity ([Brittenham, 1974](#)).

Since the neural EEG signals are always in the range of micro volts, it can be easily covered with unwanted artifacts. Typically, based on their origin, the artifact can be divided into two categories, physiological and non-physiological artifacts. The sources of physiological artifacts are the non-neural activities of the subjects, such as eye movement and muscle activities, which can hardly be avoided during monitoring. While the non-neural artifact arises from outside of the body, such as equipment and environment. This technical artifact can be reduced by proper attachment of the electrodes in a controlled environment ([Anderer et al., 1999](#)). Therefore, most of the algorithms of EEG artifact removal are developed to reduce the physiological artifacts.

In the brain computer interface (BCI) research, electrooculography (EOG) and electromyography (EMG) artifact are the most commonly detected sources of physiological artifacts.

Many studies have reported that EMG activities could affect the neurological phenomena used in a BCI system. For example, in (McFarland, Sarnacki, Vaughan, & Wolpaw, 2005), early target-related EMG artifact is presented during initial BCI training, which would be associated with unsuccessful EEG control. It is suggested that the EMG contamination should be considered in the studies using EEG rhythms. Indeed, the characteristic of frontalis and temporalis muscle EMG is described in (Goncharova et al., 2003).

2.2.1 Typical artifacts

In this section, some common types of artifacts are briefly reviewed.

Electroculogram (EOG)

Electroculogram is the electrical activity produced by eye movement, which has a large effect on EEG recording. The potential difference between the cornea and retina can be altered by eye movement, which exists not only in the wake state, but also during sleep. The strength of EOG mostly relies on the electrode close to eyes and the direction of eye movement (horizontal or vertical). In addition, the potential difference could be influenced by blinking, which is generated by the muscle movement of eye lid. This type of ocular activity produces a different waveform, and it may only occur during the wake periods. The blinking artifact has a high frequency and the amplitude is significantly larger in the frontal electrodes.

For artifact processing, EOG signals can be measured by using reference electrodes placed near the eye in practice. As a common type of artifact, EOG can present serious complication in EEG analysis due to the close proximity to the brain (Sornmo & Laguna,

2005).

Electromyogram (EMG)

Different parts of the body can be moved by the contraction of muscle tissue. These muscles are categorized as skeletal, smooth and cardiac muscles. Electromyogram (EMG) reflects the electrical activities of skeletal muscles, where the action potentials propagate between the nervous systems and the muscles. Normally, a needle electrode or non-invasively electrode could be used to measure myoelectric signals. In research practice, with the help of surface electrodes on the skin, the surface EMG is mostly investigated. The recording of surface EMG can be contaminated by different types of noise, such as electrode motion artifact, which will hinder signal quality (Sornmo & Laguna, 2005).

Cranial EMG have several properties which are responsible for the pernicious effects on the EEG background activity. First of all, it was shown that the EMG has a broad frequency distribution from 0 to >200 Hz (Goncharova et al., 2003), which means that EMG activity affects all classic EEG bands, including alpha, beta and delta bands. For topographical distribution of EMG, as the strength of muscle contraction increases, EMG effect comes to widespread and involves the entire scalp. Moreover, EMG obscures experimental manipulations in time domain, such as facial EMG, which is sensitive to cognitive and affective processes (Cohen, Davidson, Senulis, Saron, & Weisman, 1992).

The timing of muscle contraction is normally identified by using surface electromyographic (EMG) signals. Research from Conforto, D'Alessio, and Pignatelli (1999) indicated that the information acquired from this type of signal is always influenced by motion artifacts, and this disturbing effect of artifacts obstructs the correct detection and further analysis. During the non-invasive myoelectric signal recording, muscular contractions lead to the movements of electrodes, which allocate most of the artifact contribution.

Electrocardiogram (ECG)

The electrical activity of the heart is measured by electrocardiogram (ECG). Compared to the EEG signals, the amplitude of cardiac activity is lower on the scalp. The ECG interference depends on the electrode positions for certain body shapes. The normal heartbeats can usually be characterized in a repetitive, regularly occurring waveform pattern, which is helpful to reveal the presence of ECG artifact. However, when ECG is barely visible in the background EEG signals, this type of artifact may sometimes be mistaken for epileptiform activity.

Like the eye-related artifacts as we mentioned above, the ECG can be measured independently by setting several reference electrodes aside cerebral activity, which is much easier to correct EEG signals.

Technologic artifacts

As an uncontrolled/unwanted variation in the experimental setup, technologic artifacts can be generated in the data acquisition system connecting subjects to the EEG instrument, which includes the electrode, the lead, the electrode-scalp interface, the jack plug and the input cable. This type of experimental artifact could be reduced by proper procedure and planning, but it is nearly impossible to avoid or eliminate completely.

One possible source of artifact is the electrode wire which connects the electrode to the acquisition equipment. Owing to the insufficient shielding in practice, the currents flowing from nearby powerlines or electrical devices generate electromagnetic fields. Thus, 50/60 Hz powerline interference contaminates the EEG signals.

The movement of electrodes could change the DC contact potential and produce an artifact named as electrode-pop artifact. This technical artifact may occur not only in the EEG signals, but also in any bioelectric signals measured on the body surface. The electrode-pop artifact is mostly behaved as an abrupt change in the baseline level.

Motion by subjects could alter the position of the electrode on the scalp. There exists a variation of distance between the recording electrode and the skin, then a corresponding change in the electrical coupling is created and results in signal distortion. At the same time, the conduction volume between electrodes would be changed by the movement of the recording devices with respect to the underlying skin (K. Sweeney, McLoone, & Ward, 2010). It was shown that the artifact caused by electrode-scalp interface highly depends on the skin condition of subjects, as well as the type of conductive gel used. This type of artifact can be reduced through correct preparation and strong adhesion of electrodes (Huigen, Peper, & Grimbergen, 2002). Apart from that, reduction of overall movements during monitoring is an effective option. However, electrode artifact relating to motion is particularly difficult to eliminate as it does not have a predetermined narrow frequency band, and its spectrum usually overlaps with the desired signals.

2.2.2 Movement-triggered artifact

Based on the main purpose of a specific research, the actual signal of interest could be any type of the ones we described before. If the objective is to study background brain activity, then other types of signals will be regarded as unwanted interferences.

There are several kinds of movements generated by the subject during the experiment. In the past research from Tang and Zeng (2009), the body movements are divided into two groups according to the design context: design-related movements and design-stimulated movements. Design related movements are corresponding to the purpose of accomplishing the design, such as sketching, reading, typing and writing. However, the stimulated movements are aroused under the mental workload during the design process, such as scratching, moving leg, touching face and other small physical movements.

In this thesis, the artifact which we investigated includes the movement of head, leg, and the whole body. These movements involve a wide range of non-cerebral electrical

activities, and it results in the contamination of several types of artifact, such as EMG, electrode pop, electrode movement and ocular artifacts (Reis, Hebenstreit, Gabsteiger, von Tschärner, & Lochmann, 2014). As we described before, these component artifact signals have their own temporal, frequency and structural characteristics. As it is discussed in (Regan, Faul, & Marnane, 2010), which grouped artifact from head movement together for automatic artifact detection, in the similar way, the artifacts corresponding to design-stimulated movement are treated as a single class for analysis. It is assumed that this type of artifact could be differentiated from normal EEG activity.

Chapter 3

Signal Collection and Experimental Setup

In this chapter, a brief introduction of experiment is presented, from which all the EEG data are collected for analysis and further processing. The cognitive design experiment was conducted by Design Lab in 2015, and it is approved by Human Research Ethics Committee in Concordia University. The whole procedure of the cognitive experiment is designed by Thanh An Nguyen, a PhD student in our research group. The main objective of the experiment is to find out the relationship of mental effort and mental stress. To estimate cognitive effort and stress, several types of physiological signals are measured by using recording devices. Besides the EEG signals, skin conductance, heart rate and respiration were also recorded from the human body for further analysis.

3.1 Selection of participants

The participation in this experiment is voluntary. All participants with different cultural background are chosen from the Faculty of Engineering and Computer Science in Concordia University. Prior to starting the design experiment, all subjects are asked to sign the

consent form. The data used in this thesis were collected from eight healthy adults, including five males and three females with the age ranging from 20 to 35 years. All participants are right-handed and have normal eye-sight with or without glasses.

3.2 EEG signal recording

In 1947, the first international EEG congress was held in London. A placement of 10-20 electrodes system in EEG was defined by [Jasper \(1958\)](#). Since then, the 10-20 system is a traditional and widely accepted method in clinic application, thereby building a standard for comparison between subjects. The number 10 illustrates that the actual distance of adjacent electrodes in this system is 10% of the total front-back, and 20 means that the interval distance is 20% of right to left of the skull. Moreover, the name of each channel also contains necessary information. The first letter of the channel name refers to the area of the brain, and the number indicates the displacement from the midline and laterality. The central channel at the top of the scalp is named as Cz. The same definition is applied for the extended 10-10 system of electrode layout, which was accepted and endorsed as the standard of the America Electroencephalographic Society ([Committee, 1994](#)).

For EEG studies of brain activity in laboratories, a greater number of channels are used for recording and analysis. Measurement of 64 channels becomes common according to 10-10 system, and it is also what we actually used in this experiment. Nowadays, EEG helmets with up to 256 electrodes could be selected for all recording procedures. Based on the main purpose of the recording, the electrodes are placed and the number of electrodes is decided.

In this experiment, a 64-channel cap (actiCAP) is used, according to the 10-10 standard system of electrode layout. The collection of EEG signals is based on its high-quality Ag/AgCl sensors, with an easy-to-use amplifier. An open source acquisition software (PyCorder) is applied to store and display data during the experiment. Apart from EEG, other

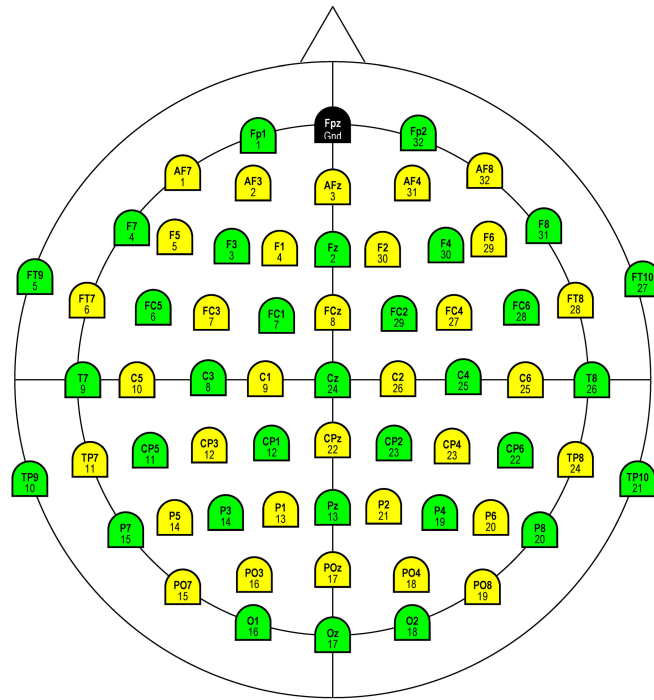


Figure 3.1: 64-Ch standard electrode layout.

sensors are applied for collecting heart rate, respiration rate and skin conductance from subjects.

To reduce the time of experiment preparation, electrodes can be plugged into the cap by experimenters in advance. Subjects are asked to wear the cap during the whole design process. There is a silt for each electrode which can inject a small amount of gel inside when the electrodes and cap are settled in place. In this way, the impedances of the EEG electrodes would be minimized. Moreover, the proper electrode paste help to stick the electrodes to the scalp.

The 64-Ch standard electrode layout is shown in Figure 3.1:

3.3 Movement recording

Since the requirement of recording method depends on the intended use, a screen-recording system is used to record the designers performance. The main purpose of recording system is to determine the occurrence of motion during design activities, and generate a time table for segmentation.

To synchronize all the video data, a digital video recorder with six cameras was chosen, as illustrated in Figure 3.2. For monitoring movements, we placed three cameras around subjects in experiment room. These three cameras were positioned at different locations to capture hand gesture, facial expression and body movements. Apart from that, another three cameras were placed in the control room, to record the designers screen display. We use a CAPTIV system to integrate electrocardiography with other physiological signals, such as skin conductance, respiration rate and heart rate, and synchronize these recording devices in time domain by sending triggers.

To keep all the physiological information associated with creativity and design process, the involvement of experimental setting and control are minimized. Participants would be positioned comfortably, and instructed to relax facial muscles. Subjects are not restricted to refrain from any physical movements, no matter the movement is necessary or not.

In order to capture body language and facial expressions of the subject, web cameras are deployed in three specific locations. The location setup of web cameras is displayed in Figure 3.3.

- Camera 1(CH3)

The first camera is placed at the left side of the subject, and it captures the sideway body, including legs and feet movements throughout the experiment.

- Camera 2(CH4)

The second camera is located at the top of computer screen to capture the facial

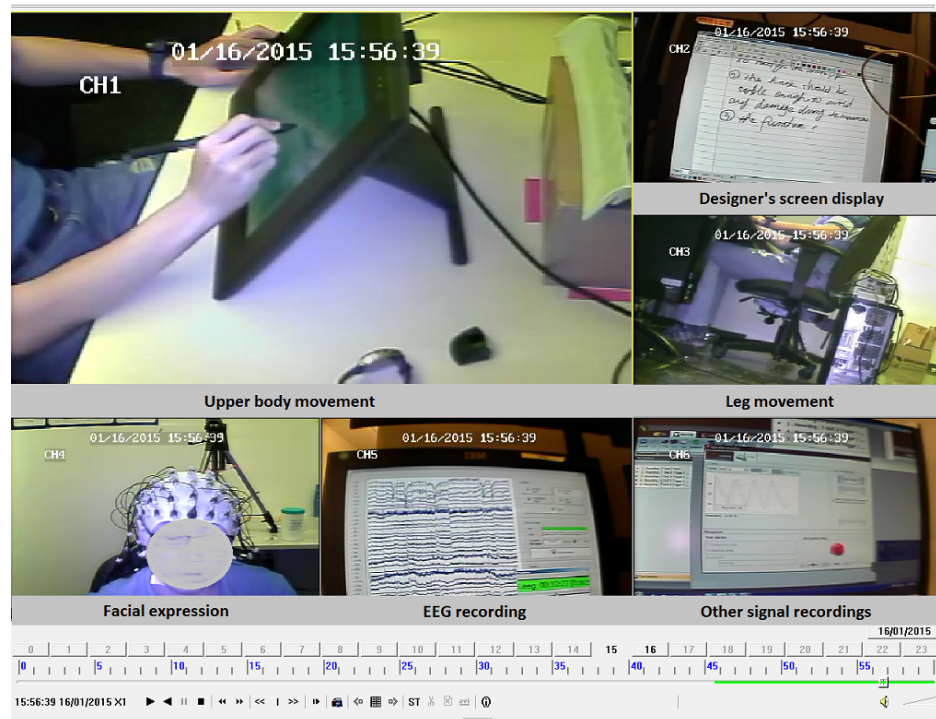


Figure 3.2: Video recording from the experiment.

expression, as well as the movements related with the subjects head. The entire face of the subject can be recorded with an adjusted angle.

- Camera 3(CH1)

The third camera is placed at the right side of the subject, and it is closer compared with the first camera. It can capture upper body movements, which include hand and arm movements, and chair movements like leaning forward and backward.

3.4 Experiment procedure

In the experiment, the subject would be given an open-ended design problem. Each subject has at most two hours for solving a design problem. All the subjects were allowed to write or sketch their solutions by using an electronic tablet, or type their answers by

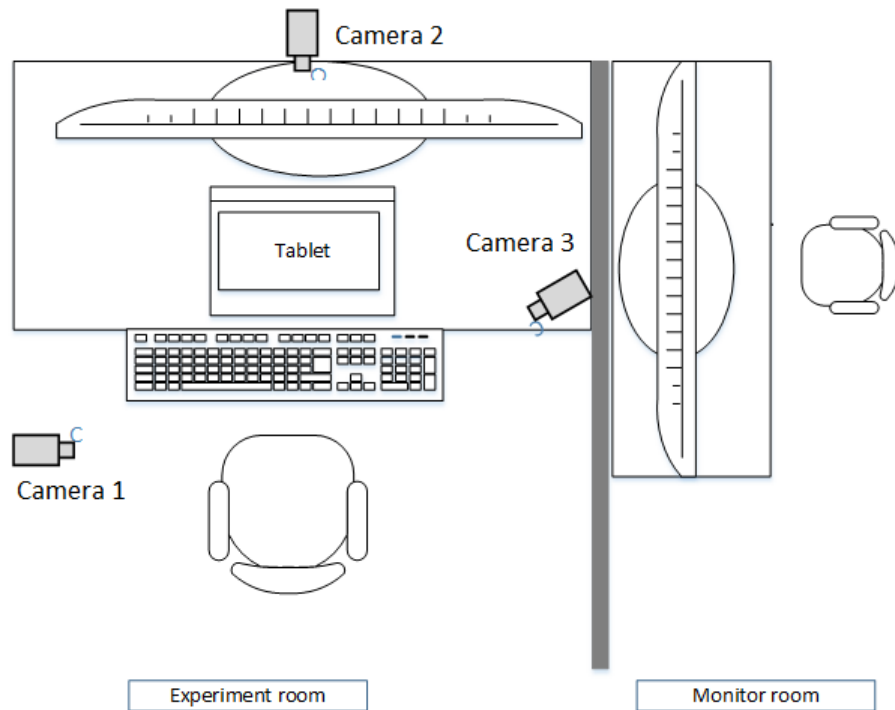


Figure 3.3: The location of three web cameras.

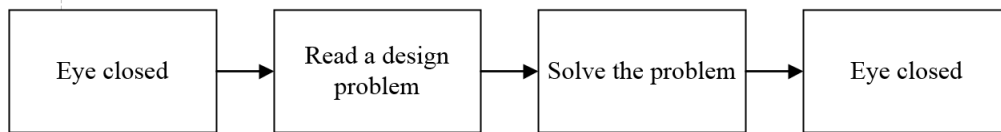


Figure 3.4: Four stages of the experiment.

keyboard. Once the experiment starts, subjects would not be interrupted by others, but they can ask for assistance if necessary. Subjects are instructed to relax and behave as normal without excessive moving.

There are four stages of design experiment, which is shown in Figure 3.4.

Stage 1: The subject is asked to seat in a comfortable armchair, and relax for three minutes with eye closed.

Stage 2: Start the design process. In this stage, the subject will be given an open task to design. For example, the subject will be asked to design a house that can be easily fly from

one place to another place.

Stage 3: After reading the information of the given problem, the subject is required to write or draw answers by using the tablet. This session is continued for a maximum period of 120 min with video monitoring. The subject is instructed to relax and behave as normal without excessive moving. Only the minimal talking is permitted.

Stage 4: After the subject completes the design problem, the subject is asked to relax for three minutes with eye closed.

The personal information of subjects and the number of segments are presented in Table 3.1.

Table 3.1: Number of segments for each subject.

Subject ID	Gender	Duration	Number of segments	Total seconds	Design problem
1	Male	0:14:01.216	6	18	Backpack
2	Female	1:07:36.044	18	66	House
3	Male	0:59:34.342	30	121	House
4	Male	0:33:05.098	7	21	House
5	Female	0:41:49.51	5	45	house
6	Male	1:40:56.346	22	100	Shoes
7	Male	0:17:36.39	4	11	House
8	Female	0:51:24.548	19	49	House

3.5 Data pre-processing

The raw EEG data is collected during the completion of the experiment, and each recording contains 64 EEG channels. The central electrode Cz was used as a common reference. Moreover, these required bio-electrical signals are sampled with a frequency of 500 Hz.

In the pre-processing unit, filtering as a simple and traditional treatment is adopted

for the raw EEG data. As described in Chapter 2.2, the non-neural artifacts usually arise from outside of the body, such as equipment and environment. In the experimental setup, an uncontrolled variation exists due to the experimental error. It is nearly impossible to completely eliminate this type of noise. While the environmental induced noises surround the human body in daily living, such as mains power leads and white noise, can be properly filtered in frequency domain by using a band-pass filter. Filtering the unwanted components will help to eliminate the majority of noises and improve signal-to-noise ratio (K. T. Sweeney, Ward, & McLoone, 2012).

In this research, to eliminate the environment noises and keep maximum information from the raw EEG data at the same time, the EEG signals were passed through a pre-defined band-pass filter, and the setting of filter is from 0.3 Hz (forward, 6 dB/oct) to 70 Hz (zero phase, 24 dB/oct). All the above preprocessing procedure has been performed in BESA software.

Chapter 4

Movement-triggered Artifact Analysis

The entire procedure for movement-triggered artifact analysis can be divided into four processing steps: preprocessing, segmentation, feature extraction/selection and comparison, as shown in Figure 4.1.

Following the pre-processing stage as described in Chapter 3, the next step is segmentation. Since the original data contains a large amount of information, and processing the whole dataset is difficult, a time period of interest needs to be selected for artifact analysis. According to the video recording of the cognitive experiment process, the segments could be created by setting boundaries at time instants corresponding to the changes of body movements. With the help of a guideline predefined for segmentation, the contaminated periods are identified by marking the exact beginning and end time of the movements.

In the next step, these extracted signals would be transformed into a set of features as reduced representation. From the previous studies, researchers analyze the EEG signals based on their features to differentiate between normal and abnormal EEG signals. Thus, the second block in this chapter named feature extraction is performed. To facilitate the interpretation of EEG signals, the characteristics of the signals is supposed to be detected and quantified through this section. The selection of features is based on the application. In this situation, the power in the beta band may be relevant to muscle artifact.

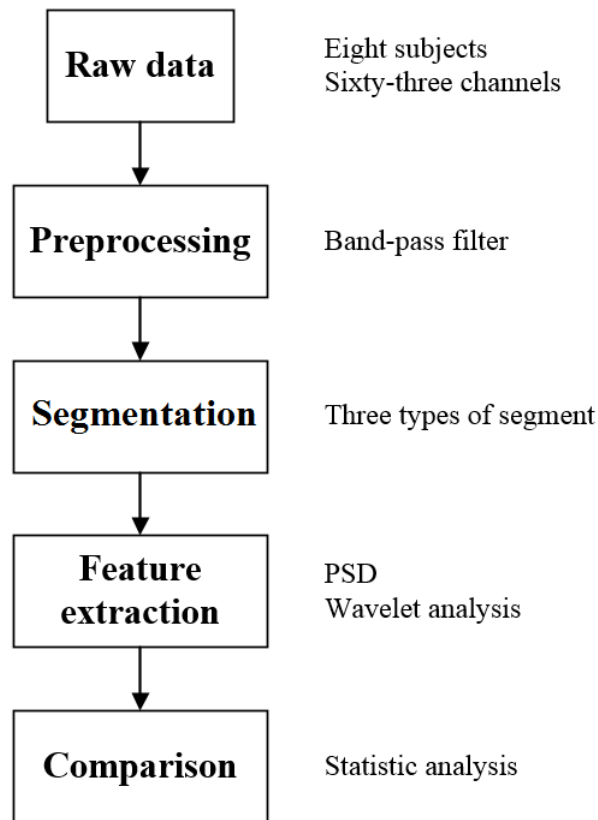


Figure 4.1: The overview of movement-triggered artifact analysis.

During artifact analysis section, we mainly present a guideline to segment the raw EEG signals. After that, the calculation of several parameters are presented for feature extraction. In this way, EEG on the basis of its features in frequency domain is investigated.

4.1 EEG data segmentation

In the visual inspection of segmentation process, one observer is involved to mark the movement-triggered segment accurately, who processes the same data twice to make sure the beginning and the end of marking is reliable. All the video recording were displayed in a computer software named Playback, and the EEG recording is performed in PyCorder software showing all the channels page-by-page, each lasting 10 seconds.

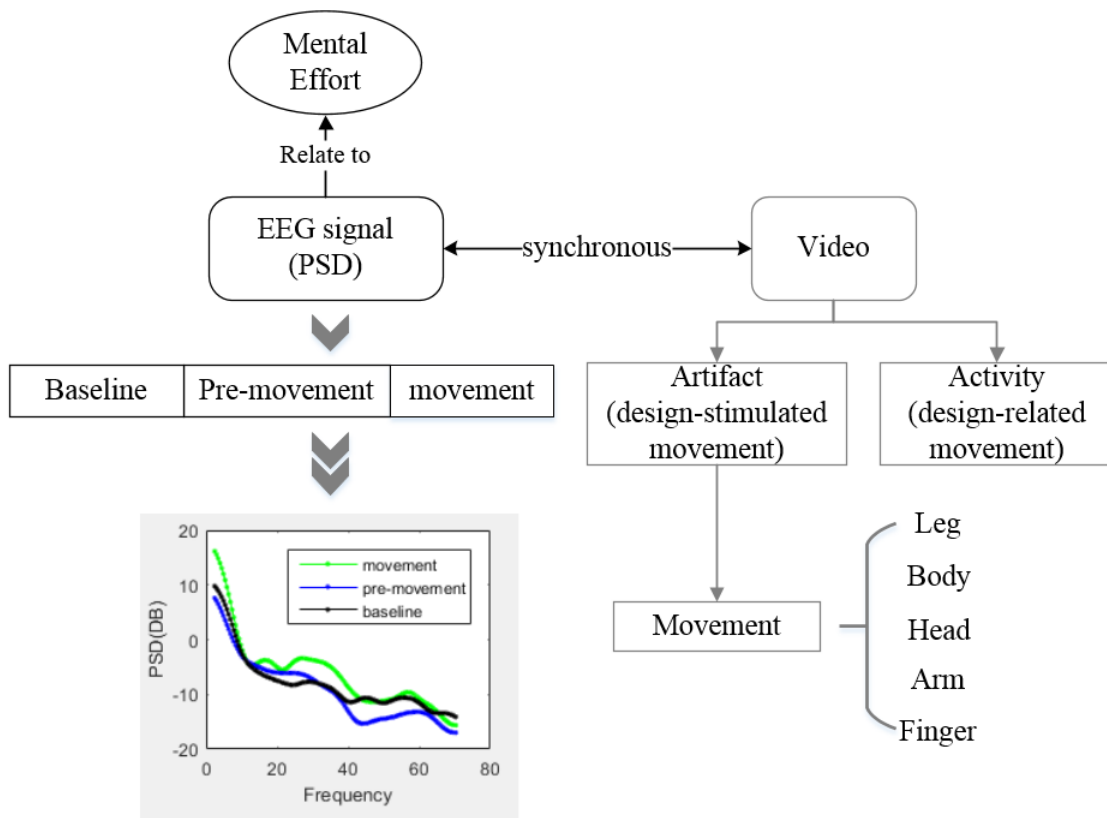


Figure 4.2: Segmentation process and relation between video and EEG.

Figure 4.2 shows the structure of segmentation process and the relation between video recording and EEG signals. After monitoring the whole process of experiments, the physical motions generated by experimenters would be divided into two categories. One is the body activities related to completing design objectives, which is essential and unavoidable when solving the given problems. The other one is the involuntary movements, which are accompanied with the cognitive process. Actually, the first type of activity cannot be avoided, and it always lasts for a period of time, such as typing. For this reason, we mainly focus on the latter one, which normally has a quite short length for analysis. This type of involuntary movements can be generated from various sources of subjects, including legs, feet and head.

To extract the segments of movement-triggered EEG signals, we define a set of criteria as following:

- Subjects should be in any stage of design process as defined in Chapter 3. There should be a minimum of ten continuous seconds before a movement-triggered signal could be segmented.
- The movement generated by the subject should have a duration of at least 2 seconds or greater to be marked as movement-triggered EEG signals.
- A minimum of ten continuous seconds of interval is required to segment a second movement-triggered epoch.
- The occurrence of movements should be considered only if the movement is significant in the video and unrelated with output of the design process. As we discussed in section 2.2.3, where we define the movements for analysis, several typical movements would be recorded, including leg movement, head movement and body movement.

In general, this segmentation guideline is not a strictly defined procedure, and it also allows subjectivity in capturing movement artifacts. In this research, we use large-scale physical movements which can be identified by the video recording. The start time and end time are recorded in the time table along with a brief behavior description. Table 4.1 shows part of the time table of body movements, which is used to extract movement-triggered segments for further analysis.

After marking the segments when movements occur, we extract two more segments as well, in order to investigate the transition from non-movement state to movement one. When we compare the differences of these two states, inter-subject variability is supposed to be reduced by using reference. Therefore, we define three types of segments for investigating the impact of body movement on EEG signals. Figure 4.3 illustrates how these

Table 4.1: Time table of physical movements for segmentation

Movement No.	EEG recording		Duration (seconds)	Description of movements
	Start time	End time		
1	0:07:44	0:07:50	6	move body
2	0:09:16	0:09:21	5	move body
3	0:10:04	0:10:08	4	move body
4	0:11:55	0:11:58	3	move leg
5	0:12:51	0:12:56	5	move leg, body slightly
6	0:13:35	0:13:38	3	move body
7	0:19:34	0:19:36	2	move leg (a little)
8	0:20:59	0:21:02	3	move body (swivel in the chair)
9	0:22:35	0:22:37	2	move body (swivel in the chair)
10	0:25:59	0:26:02	3	move leg, then move body by swiveling the chair
11	0:26:32	0:26:37	5	move body (swivel in the chair)
12	0:28:35	0:28:37	2	move body (swivel in the chair)
13	0:38:58	0:39:01	3	move body (swivel in the chair)
14	0:39:47	0:39:49	2	move leg (a little)
15	0:53:29	0:53:31	2	move body (swivel in the chair) slightly
16	1:00:29	1:00:38	9	move body (swivel in the chair) largely, move leg
17	1:03:15	1:03:20	5	move body (swivel in the chair) slightly
18	1:04:35	1:04:38	3	move leg

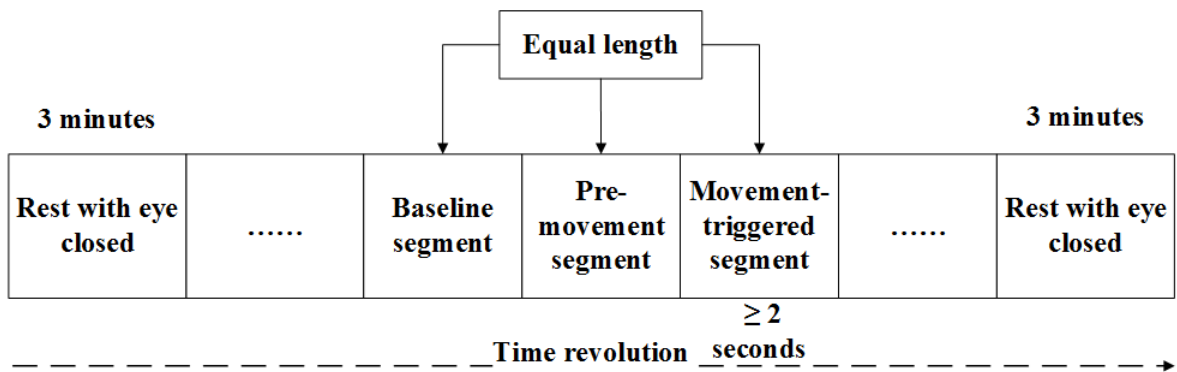


Figure 4.3: Three types of segments in the time domain.

segments obtained from a sample movement trial in the time domain.

(1) Movement-triggered segment

Based on the video, the specified EEG epochs during each movement of the subject are collected. The length of each epoch could be different, and there exist different types of movement generated by the subjects.

(2) Pre-movement segment

A pre-movement is an epoch happening just before its corresponding movement, and they both have the same length of time.

(3) Baseline segment

Before pre-movement segment, the same length of EEG signal is extracted as the baseline of this movement.

4.2 Feature extraction in artifact analysis

Recently, numerous different methods have been applied to extract diverse features from EEG signals. Five of the well-known methods in frequency domain and time-frequency

domain have been discussed (Al-Fahoum & Al-Fraihat, 2014), which are time frequency distributions (TFD), fast Fourier transform (FFT), eigenvector methods (EM), wavelet transform (WT) and auto-regressive method (ARM). After comparing their performances, it is indicated that there does not exist an optimum method for all applications.

To increase the computational efficiency and get some basic information in artifact analysis, we narrow down the number of channels in the first step. According to the 64-Ch standard electrode layout for actiCHamp, the six channels C3, C4, P3, P4, P7, P8 which are usually used for detecting muscle artifact are selected for data comparison (Van de Velde, van Erp, & Cluitmans, 1998). For each channel, the absolute power of different frequency bands can be obtained in each type of segment. After that, the same procedure will be repeated for all other 57 channels except the reference channel Cz for statistical analysis.

4.2.1 Power spectral analysis

In frequency domain, the power spectral density is a widely-used method to describe the power intensity of the signal. Power spectral analysis transforms a signal from time domain to frequency domain, and characterizes the relationship between amplitude and frequency. Almost all the available spectral analysis techniques are based on the Fourier transform, whose inverse also allows the signal to be recovered from the transformed one. The discrete Fourier transform (DFT) decomposes a signal into its frequency components, as expressed by Eq. (1):

$$DFTx(n) = X(k) = \sum_{n=0}^{N-1} x(n)e^{(-j\frac{2\pi}{N}nk)} (0 \leq k \leq N - 1) \quad (1)$$

The inverse discrete Fourier transform is given by Eq. (2):

$$IDFT\{x(k)\} = X(n) = \frac{1}{N} \sum_{k=0}^{N-1} X(k)e^{(j\frac{2\pi}{N}nk)} (0 \leq n \leq N - 1) \quad (2)$$

In practice, the Fast Fourier transform (FFT) is often used for fast computation of the DFT. When the data is deterministic with no random effects, a Fourier transform is directly performed to decompose the signal into a sum of sinusoids of different frequencies. However, the real signal is always obscured by unwanted noise. To obtain the desired features while suppressing the noise, the PSD estimation is often calculated through efficient methods, such as averaging or smoothing. In general, there are two main methods for power spectral density estimation, non-parametric and parametric.

Parametric methods typically set signal models with assumption to calculate power spectral density estimate. Based on linear prediction, the autoregressive (AR) method is frequently used in practice for the ease of computing PSD through AR coefficients. The autoregressive method performs well in moderate-to-high SNR ranges, for narrowband signals, the performance of this method highly depends on the model order selector. If the model order is too small, the spectrum will lack resolution and have a highly smoothed effect. If the order selected is too high, false peaks would then occur.

For a wide-sense stationary process, the power spectral density cannot be consistently estimated from periodogram. Therefore, Welch's technique (Welch, 1967) is introduced as a non-parametric method to estimate PSD. To reduce the variance of the periodogram, this method breaks the time series into segments, each segment being multiplied by a window function, such as Hamming window. Then, a modified periodogram is computed for each segment, and all the resulting periodograms from different segments are averaged to estimate the power spectral density. The segments usually overlap to avoid the information loss caused by windowing (Solomon Jr, 1991). This method is briefly explained as follows.

We assume $x(0), x(1), \dots, x(N-1)$ as a signal in time domain, and partition the data sequence into K segments of length M . The k -th segment can be denoted as $x_k(i), i = S, \dots, M + S - 1$ where S is the shift points between segments. The windowed discrete

Fourier transform (DFT) is computed as:

$$X_k(f) = \sum_m x_k(m)W(m)e^{(-2\pi j)(mf)} \quad (3)$$

where $m = S(k - 1), \dots, M + S(k - 1)$ and $W(m)$ is the window function.

The modified periodogram for each segment $P_k(f)$ is then calculated as:

$$P_k(f) = \frac{1}{W} |X_k(f)|^2$$

$$W = \sum_{m=0}^M [W(m)]^2 \quad (4)$$

At last, we obtain Welch's estimate of PSD by averaging the periodogram values:

$$PSD(f) = \frac{1}{K} \sum_{k=1}^K P_k(f) \quad (5)$$

In this thesis, Welch's method is applied to estimate the power spectra with a Hamming window of 1-second duration with 50% overlap since EEG signal is non-stationary. Figure 4.4 shows the PSD of one channel, computed for movement-triggered segment, pre-movement segment and baseline segment.

In order to distinguish the movement-triggered segments and no-movement segments, several parameters in the frequency domain are chosen:

- (1) Total power in 4-30 Hz

In this thesis, the total power is defined as the band power in frequency interval of 4 to 30 Hz. The frequency below 4 Hz is not included in the calculation of total power.

- (2) Relative power in Beta2 band

The relative power is defined as the percentage of the total power in this specified frequency interval. It is reported that Beta activity mostly occurs during active thinking.

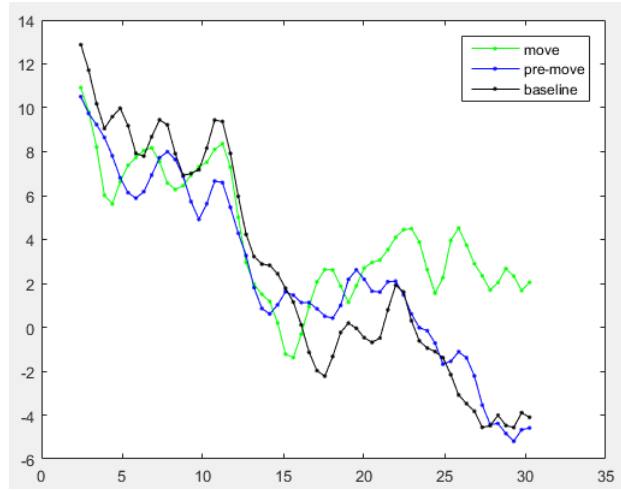


Figure 4.4: Power spectral density (PSD) of one subject in a specific movement.

Considering the extension of individual alpha frequency (Goljahani et al., 2012), a high Beta range from 20 to 30 Hz is selected for measuring mental effort (Nguyen & Zeng, 2016). The relative Beta2 band power can be computed as the ratio of its band power to the total power, which is described as Eq. 6.

$$R_{Beta2} = \frac{P_{Beta2}}{P_{total}} \quad (6)$$

where P_{Beta2} is the average power computed by integrating the power spectral density estimate over the Beta2 band.

(3) 95% Spectral edge frequency (SEF)

The 95% spectral edge frequency is defined as the frequency below which 95% of the total power resides, which can be used to reflect the shift in EEG signals from low (high) frequency to high (low) frequency.

Spectral edge frequency is investigated to describe the presence of movement-triggered artifacts. In clinical practice, SEF has been used to measure the depth of anesthesia

and indicate intra-operative movements (Schwender et al., 1996). Besides, as a frequency domain parameter, SEF is applied to detect short periods muscle artifacts automatically in normal awake EEG signals (Van de Velde et al., 1998).

4.2.2 Wavelet analysis

Based on the uncertainty principle, when the window size gets narrow, the frequency resolution becomes poor, and vice versa. As the signals we applied are localized with quite short length in time series, similar with ERP components, their power spectral analysis based on short-time Fourier transform has limited performance. For this reason, wavelet is proposed as an effective technique dealing with transient signals, which exploits the information from both time and frequency domains. Also, there is no assumption for the stationarity of the recorded signals. Moreover, wavelet transform can be used in many domains of bio-signal processing, such as the seizure epileptic diagnosis (Adeli, Zhou, & Dadmehr, 2003) (Guo, Rivero, Seoane, & Pazos, 2009) (Kumar, Dewal, & Anand, 2012) and the classification of movement-related cortical potentials (MRCPs) (Farina, do Nascimento, Lucas, & Doncarli, 2007).

The wavelet transform decomposes a signal into a set of basic functions called wavelets. A signal in general can be considered as a superposition of different structures occurring on different time scales at different times or spatial scales at different locations. A set of elementary functions can be applied as mother wavelets for decomposition of original signals. Examples of traditional wavelets are Haar and Daubechies wavelets. As the main base of wavelet transform, the selection of mother wavelet function will affect the precision for identifying the desired signals.

In general, two types of wavelet analysis exist in data processing, namely continuous wavelet transform (CWT) and discrete wavelet transform (DWT). The continuous wavelet

transform (CWT) of a signal $x(t)$ is defined as Eq.7:

$$CWT(a, b) = \int_{-\infty}^{\infty} \frac{1}{\sqrt{|a|}} x(t) \Psi\left(\frac{t-b}{a}\right) dt \quad (7)$$

where a and b are the scale and shifting parameters, respectively. The wavelet becomes narrower when the value of a increases.

When $a = 2^j$ and $b = 2^j k$, we have

$$CWT(a, b) = \int_{-\infty}^{\infty} \frac{1}{\sqrt{|2^j|}} x(t) \Psi\left(\frac{t-2^j k}{2^j}\right) dt \quad (8)$$

According to Nyquist rule, the raw signal is down-sampled by two and the output signal has maximum one-half of the frequency bandwidth.

Multi-resolution representation provides an effective way of implementing DWT (Mallat, 1989). This decomposition is computed with a pyramidal algorithm based on convolutions by quadrature mirror filters, which contain a series of high-pass (HP) and low-pass (LP) filter pairs. In DWT filter implementation, the output signal of high-pass filter corresponds to the detailed wavelet coefficients, and low-pass filter produces the approximation coefficients of each level. The whole process of decomposition is illustrated in Figure 4.5.

The frequency bands of signal component $D_j(k)$ and $A_j(k)$ can be obtained as:

$$\begin{aligned} D_j(k) &: \left[\frac{f_s}{2^{j+1}}, \frac{f_s}{2^j} \right] \\ A_j(k) &: \left[0, \frac{f_s}{2^{j+1}} \right] \end{aligned} \quad (9)$$

where $j = 1, 2, \dots, J$

The approximation and detailed coefficients could provide information of the signal in different frequency bands. Each band is defined according to the level of decomposition and the sample rate of the original EEG signals.

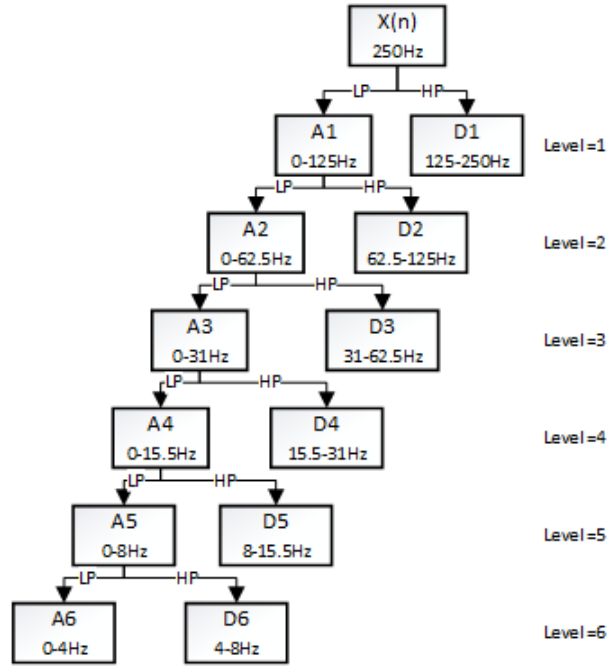


Figure 4.5: EEG signal decomposition based on DWT.

Wavelet entropy

Wavelet entropy is an alternative method to study the irregularity of signals, which is calculated based on the energy distribution in the wavelet sub-bands. Considering the different length of movement-triggered segments, the mean wavelet energy is considered for feature extraction instead of using the total wavelet energy. At resolution level j , the mean wavelet energy of detail coefficients is defined as:

$$\bar{E}_j = \frac{1}{N_j} \sum_{k=1}^j |D_j(k)|^2 \quad (10)$$

where N_j is the number of wavelet coefficients at level j .

Then, the total mean energy for the segment will be:

$$E_{total} = \sum_{j=1}^N E_j \quad (11)$$

The relative wavelet energy in time evolution is calculated by:

$$p_j = \frac{E_j}{E_{total}} \quad (12)$$

The wavelet entropy for each channel r can be obtained by:

$$WE_r = - \sum_{j=1}^N p_j \ln(p_j) \quad (13)$$

The wavelet transform-based entropy not only measures the degree of order (disorder) of signal segments, but also reflects the underlying dynamical process in consequence (Rosso, Blanco, & Figliola, 2004).

Relative wavelet entropy

As described before, the wavelet entropy of each segment can be calculated straightforwardly. To measure the degree of similarity between two segments on the other hand, the so-called relative wavelet entropy was introduced in (Rosso et al., 2001) as well.

The probability distribution of the wavelet energy for two EEG segments could be represented as $\{p_j\}$ and $\{q_j\}$, with $\sum_j p_j = \sum_j q_j = 1$. The relative wavelet entropy is then calculated as

$$R_{WT}(p|q) = \sum_{j=1}^N p_j \ln\left(\frac{p_j}{q_j}\right) \quad (14)$$

where the distribution $\{q_j\}$ is taken as a reference distribution. If $p_j \equiv q_j$, the RWE vanishes.

4.3 Experimental results

EEG recording is a mixture of underlying brain potentials and additional waveforms. Considering the main purpose of this research, the actual signal of interest is movement-triggered artifact during cognitive tasks. In most circumstances, this type of artifacts are identified from raw data after the contaminated channels or epochs are rejected through visual inspection, and characterized for further detection and removal. In recent studies, some efforts have also been made to separate artifacts from scalp EEG. For example, a non-conductive layer (a silicone swim cap) is placed over the scalp of subjects, in order to block electro-physiological signals from electrodes, and thus directly record the movement artifact signals during walking (Kline, Huang, Snyder, & Ferris, 2015). During design activities, however, the movements generated by subjects are unpredictable in advance and hardly repeatable, and therefore we cannot isolate and record the movement-triggered artifact for further analysis. For this consideration, we examine the following two types of consecutive periods from raw data to perform the variability tracking, named as test period and context period, respectively. In the test period, the statistical significance is examined by comparing the variances of movement-triggered and pre-movement segments. In the context period, the variances of pre-movement and baseline segments are compared for statistical analysis.

A graphical user interface (GUI) is developed in Matlab to analyze EEG signals from eight subjects, as shown in Figure 4.6. Figure 4.7 indicates the power spectral density of movement 5 (Subject 3) in frontal lobe.

4.3.1 Results using relative Beta2 power

Figure 4.8 shows that the average relative Beta2 power for six channels in three types of segments. For all subjects, it can be observed the mean value in movement-triggered segment is always greater than the other two types of segments. For the variance of relative

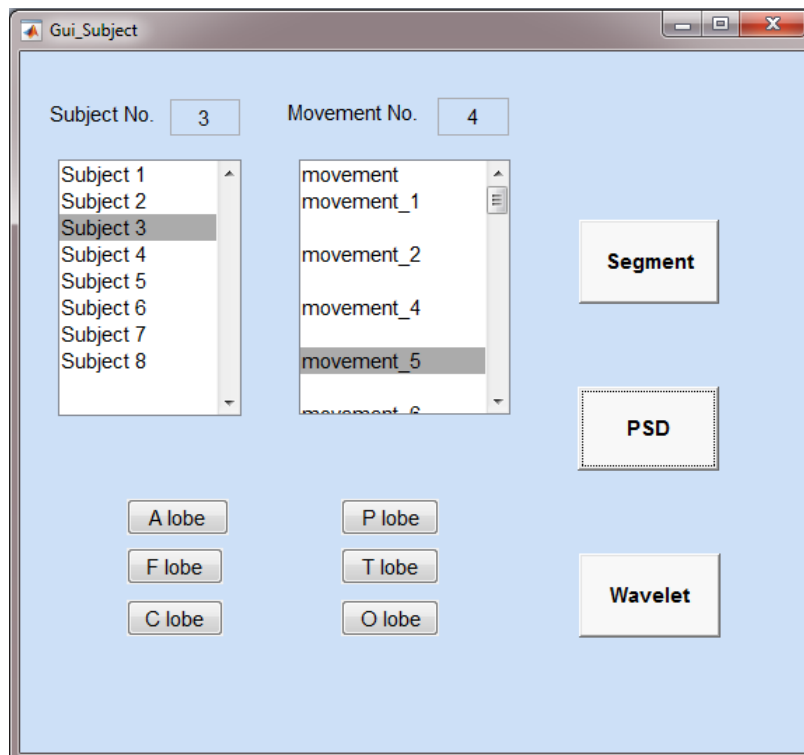


Figure 4.6: A graphical user interface (GUI) for data analysis.

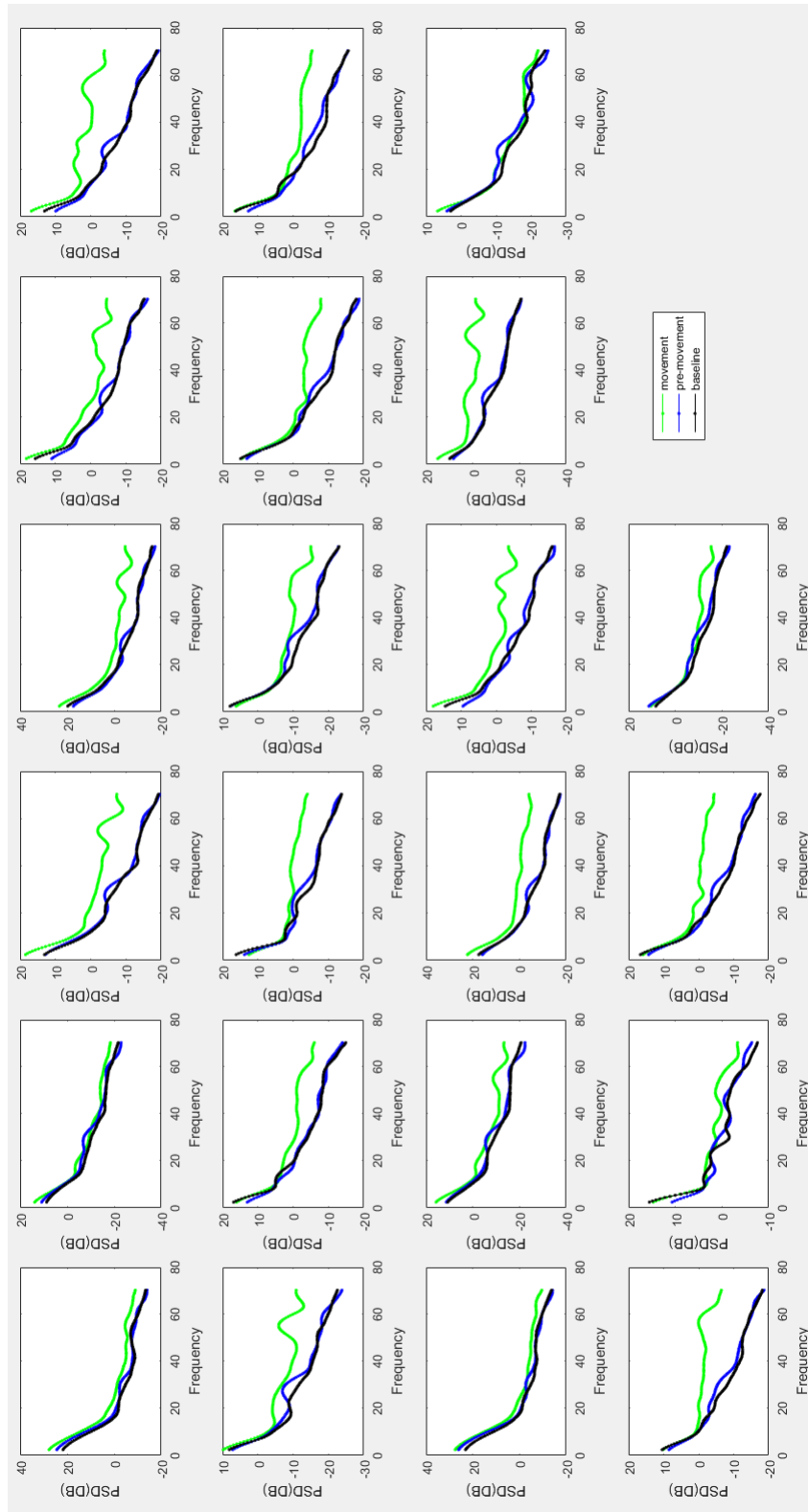
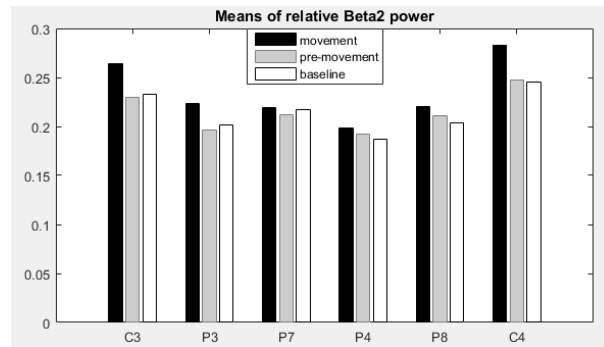
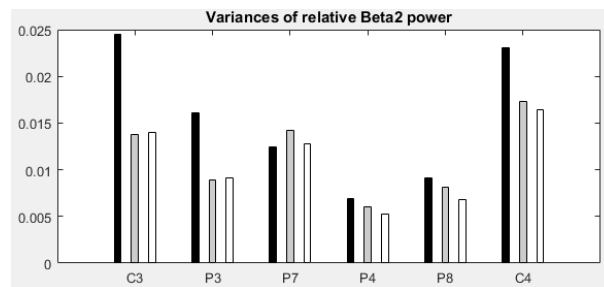


Figure 4.7: An example of PSD in graphical user interface (GUI).



(a)



(b)

Figure 4.8: Comparison of means (a) and variances (b) of relative Beta2 power for each channel.

Beta2 power, five channels have higher variances in movement-triggered segment except P7, compared with pre-movement and baseline segment.

By using Wilcoxon signed rank test for all six channels, a significant difference in the relative Beta2 power medians between pre-movement segments and movement-triggered segments can be observed in C4 channel at the 5% significance level. It can also be concluded by statistic evidence that the median relative Beta2 power in movement segments is greater than the median value in pre-movement segments. However, there is no significant difference in relative Beta2 power at both test period and context period in the other five channels (C3, P3, P7, P4 and P8).

The statistical analysis is also applied to all channels, and the result is shown in Figure 4.9, with p-value presented in Table 4.2. The colored channel reflects that there is a significant difference in the relative Beta2 power between the movement-triggered segments and

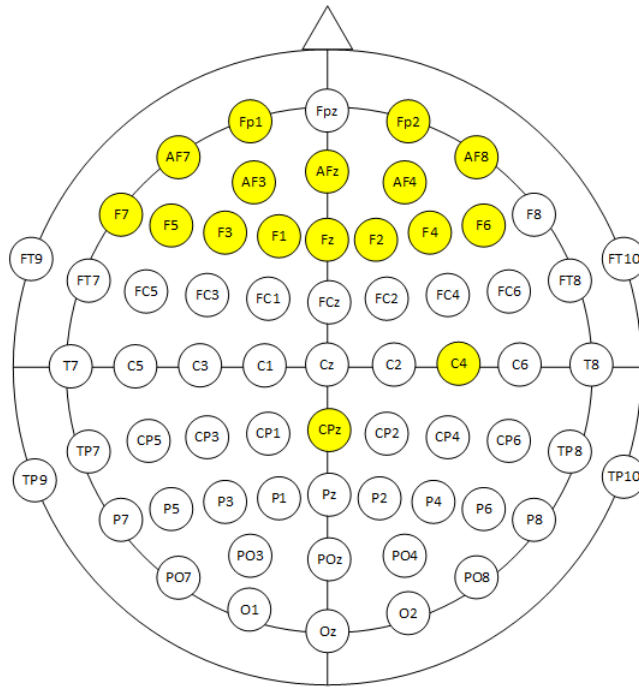


Figure 4.9: Statistical analysis of relative Beta2 power for all channels.

the pre-movement segments, while other non-colored channels accept the hypothesis of no difference. Among them, movements mainly affect the power spectral amplitude in Beta2 frequency range at the anterior scalp locations.

As for spectral edge frequency (SEF), after applying Wilcoxon signed rank test, the result is shown in Figure 4.10 (P-value in Table 4.3). It can be seen that there exist significant differences in the median values of SEF between the movement-triggered segments and pre-movement segments (in test period) at the 5% significance level, and it is mostly located at the anterior scalp as well.

Among all the investigated conditions, the inter-trial EEG activity has the possibility to be affected by various types of movements, and it will modify the relative quantifiers in return. To further explore the possible influence of movement types on extracted features, the movements generated by subjects are divided into four categories, which are leg, face, body and head movements respectively. The grand average of relative Beta2 power for all

Table 4.2: P value for colored channels in test period (Beta2).

Channel Name	Fp1	Fz	F3	F7	C4	F4	Fp2	AF7	AF3
P-value	4.25E-06	0.01074	0.01413	0.00424	0.03464	0.00673	9.68E-05	4.96E-05	1.53E-06
Channel Name	AFz	F1	F5	CPz	F6	F2	AF4	AF8	
P-value	8.06E-05	0.02946	0.00129	0.04058	0.00543	0.03291	2.94E-05	3.61E-05	

Notes: 5% Significance level

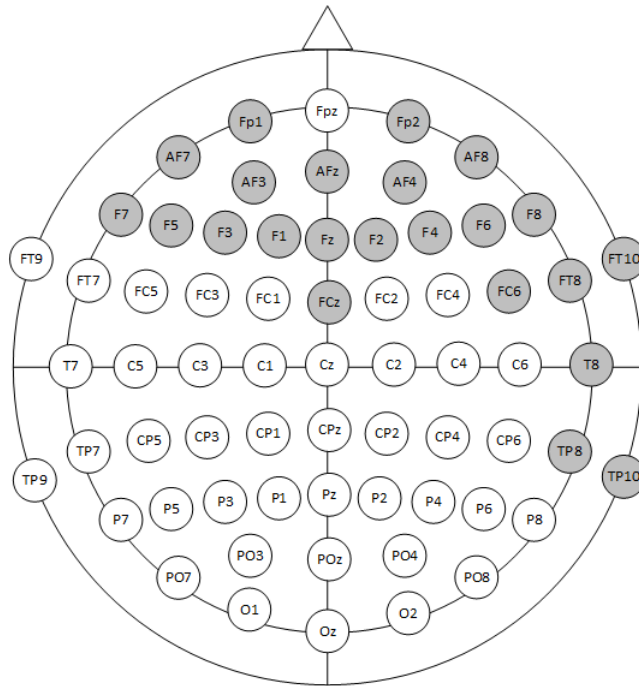


Figure 4.10: Statistical analysis of spectral edge frequency (SEF) for all channels in test period.

Table 4.3: P-value for colored channels in test period (SEF).

Channel Name	Fp1	Fz	F3	F7	TP10	T8	FT10	FC6
P-value	3.96E-07	0.00072	0.00599	0.00577	0.00034	0.00037	0.00160	0.03455
Channel Name	F4	F8	Fp2	AF7	AF3	AFz	F1	F5
P-value	0.00440	0.00193	8.50E-10	0.00054	9.63E-07	3.15E-07	0.00206	0.00362
Channel Name	FCz	TP8	FT8	F6	F2	AF4	AF8	
P-value	0.01669	2.46E-05	0.00168	0.00080	0.00317	6.67E-09	6.75E-06	

Notes: 5% Significance level

channels is shown in Figure 4.11.

4.3.2 Results using wavelet entropy

Figure 4.12 shows the mean and variance of wavelet entropy for all six channels, and the comparison in three types of segments. The result illustrates that the variance value of WE is significantly larger when the movement occurs. Statistical analysis is also performed by Friedman test, and no significant difference exists between wavelet entropies for the three segments.

Since the relative wavelet entropy is a quantitative method to measure the degree of similarity between different segments of the EEG signal, the RWE in the test period and that in the context period are compared to identify the transition when movement occurs. For all channels, the significant difference distribution of RWE is illustrated in Figure 4.13.

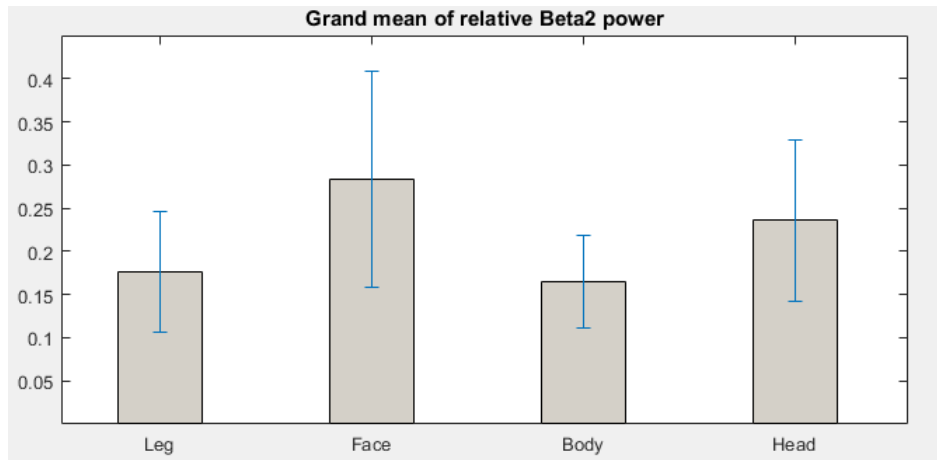
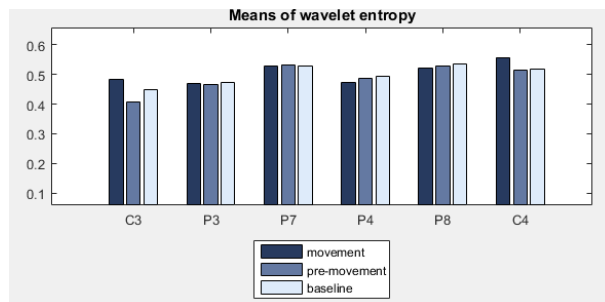
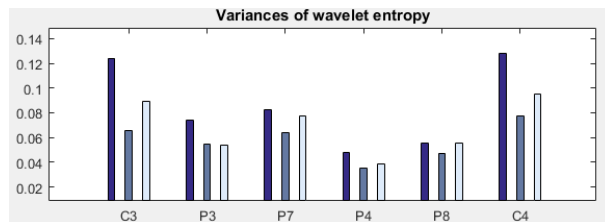


Figure 4.11: Grand mean of relative Beta2 power in four types of movements.



(a)



(b)

Figure 4.12: Comparison of means (a) and variances (b) of wavelet entropy for three types of segments.

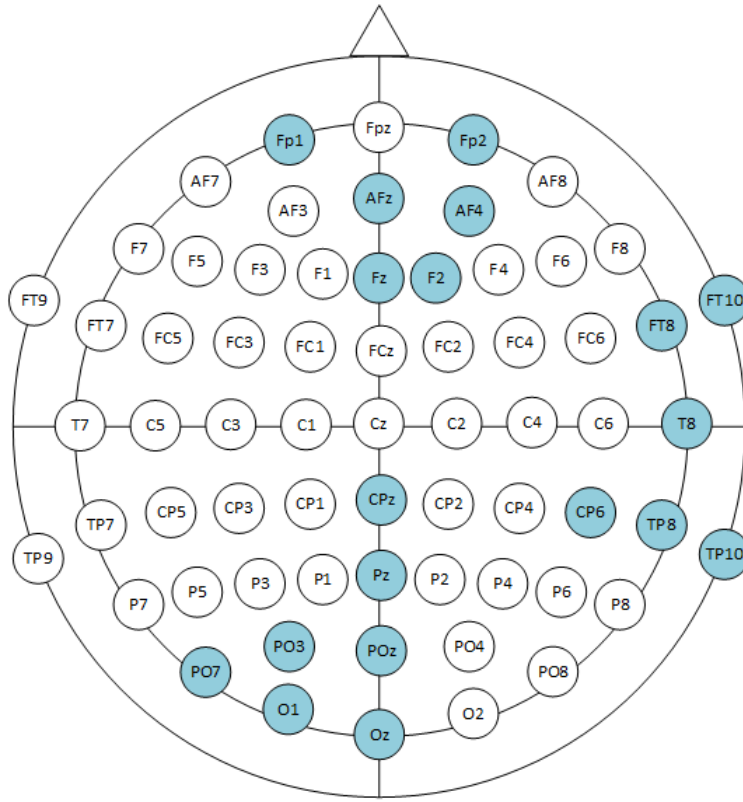


Figure 4.13: Statistical analysis of relative wavelet entropy (RWE) for all channels.

Table 4.4: P value for colored channels in test period (RWE).

Channel Name	Fp1	Fz	Pz	O1	Oz	TP10	CP6	T8	FT10	Fp2
P-value	0.00831	0.02554	0.00424	0.00482	0.01178	5.91E-05	0.04116	0.00040	0.00655	0.03592
Channel Name	AFz	PO7	PO3	POz	CPz	TP8	FT8	F2	AF4	
P-value	0.04606	0.01484	0.02733	0.01622	0.01111	0.02946	0.02294	0.03644	0.04145	

Notes: 5% Significance level

Chapter 5

Artifact Removal

Actually, it is nearly impossible to avoid the occurrence of ocular and muscle activity in monitoring brain signals. In clinical practice, the most direct approach is the rejection of entire contaminated data segments. Based on the expertise of experts, the trials are checked visually and removed from the analysis. This method mostly relies on human experts or well-trained experimenters who can identify all types of artifact epochs from the original recording, so as to make sure the data applied in analyses represent real brain activity. However, there exist many disadvantages with rejection of contaminated EEG segments. The first one is that the selection of artifact may be subjective, thus, it is usually affected by the expert performance. At the same time, it is a time consuming task, especially for a large amount of recorded data. Moreover, the biggest problem of manual rejection is a substantial information loss, which could cause a huge drawback on the analysis section and consequently reduce the quality of desired data. To overcome these drawbacks, several automatic artifact removal approaches have been proposed in recent studies.

The raw signal recorded from the experiment is $X(n)$, which is a combination of the underlying brain activity $R(n)$ and the unwanted noise $N(n)$, as illustrated in Figure 5.1. The function f describes how the artifact modifies the desired signal, which contains additive or multiplicative artifacts. While additive artifact is predominantly considered because it

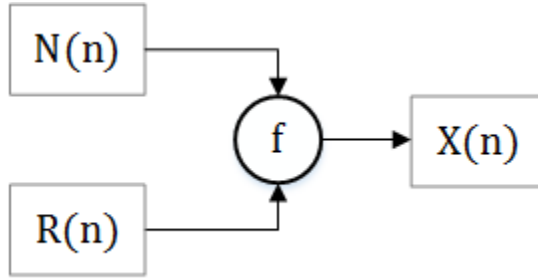


Figure 5.1: General framework of signal combination.

is easy to handle in practice. Also, the majority of artifact removal techniques assume that the number of sources should be equal or smaller than the recorded channels, especially for blind source separation techniques.

In this chapter, two commonly used algorithms are reviewed for artifact removal, namely, canonical correlation analysis (CCA) and independent component analysis (ICA). The experimental procedure of movement-triggered artifact removal is shown in Figure 5.2.

5.1 Canonical correlation analysis (CCA)

In blind source separation by canonical correlation analysis (BSS-CCA) for artifact removal, the contaminated EEG signal is generated by both brain source and muscle activity. It assumes these sources are uncorrelated and maximally auto-correlated. Compared with brain activity, muscle artifact always has relative low autocorrelation. Therefore, BSS-CCA can separate the muscle and brain activity sources and remove the movement-triggered artifact (Clercq et al., 2006).

Let $X(t)$ be the raw data in time domain, which is represented as:

$$X(t) = [x_1(t), x_2(t), \dots, x_R(t)]^T (t = 1, \dots, N) \quad (15)$$

with N being the number of sample points and R the number of channels. We assume the

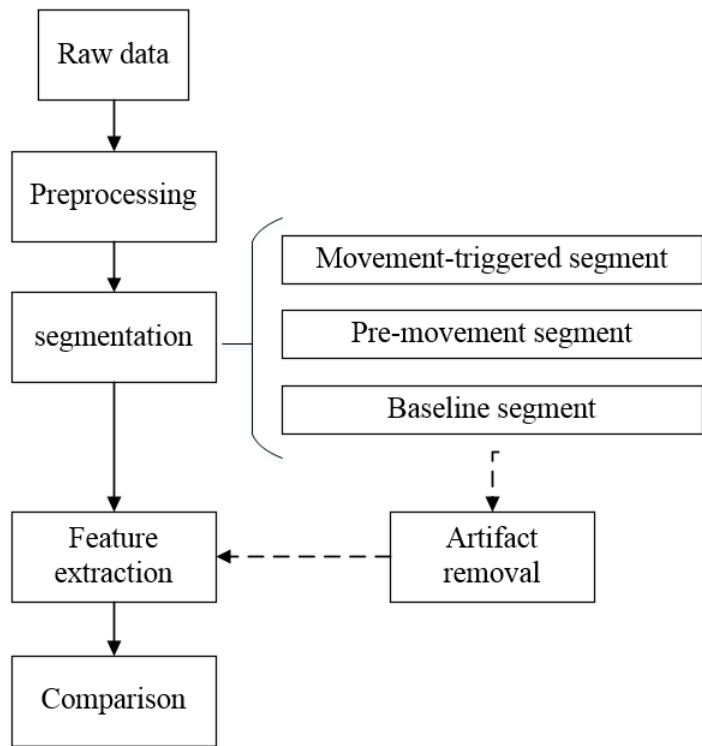


Figure 5.2: Experimental procedure of movement-triggered artifact removal.

EEG raw signal recorded from the experiment is an unknown mixture of a set of source signals $S(t) = [s_1(t), s_2(t), \dots, s_R(t)]^T$, with equality number of sources and channels, and linear mixing. The raw data can be obtained by a matrix multiplication:

$$X(t) = MS(t) \quad (16)$$

where M is an unknown mixing matrix. To recover the source signals $S(t)$, the mixing matrix should be estimated beforehand. It can be obtained by introducing de-mixing matrix A as:

$$S(t) = AX(t) \quad (17)$$

Normally, A is the inverse of the mixing matrix M from the previous equation.

Let $Y(t)$ be a temporal delayed matrix of the raw data $X(t)$ with one sample lag, represented as $Y(t) = X(t - 1)$. Considering the linear combination of the source components for $X(t)$ and $Y(t)$, the variates are defined as:

$$\begin{aligned} u &= a_{x_1}x_1 + \dots + a_{x_R}x_R = a_x^T X \\ v &= a_{y_1}y_1 + \dots + a_{y_R}y_R = a_y^T Y \end{aligned} \quad (18)$$

where $a_x = [a_{x_1}, \dots, a_{x_R}]^T$ and $a_y = [a_{y_1}, \dots, a_{y_R}]^T$ are the weight vectors.

Since the sources are supposed to be maximally auto-correlated, the correlation ρ between u and v also need to be maximized as below to meet the assumption:

$$\max_{a_x, a_y} \rho(u, v) = \frac{E[uv]}{\sqrt{E[u^2]E[v^2]}} = \frac{a_x^T C_{xy} a_y}{\sqrt{(a_x^T C_{xx} a_x)(a_y^T C_{yy} a_y)}} \quad (19)$$

where C_{xx} and C_{yy} are the autocovariance matrix of X and that of Y , respectively, and C_{xy}

is the cross-covariance matrix of X and Y . After some manipulations, we obtain

$$\begin{cases} C_{xx}^{-1}C_{xy}C_{yy}^{-1}C_{yx}\hat{a}_x = \rho^2\hat{a}_x \\ C_{yy}^{-1}C_{yx}C_{xx}^{-1}C_{xy}\hat{a}_y = \rho^2\hat{a}_y \end{cases} \quad (20)$$

The square root of the eigenvalue is the canonical correlation coefficient ρ , and the eigenvectors are a_x and a_y . Actually, X and Y contain almost the same data, so the same data is also contained in a_x and a_y . Therefore, solving a_x is sufficient. The first variates are constructed and the relation between $u_1(t)$ and $v_1(t)$ is:

$$v_1(t) = a_y^T Y(t) = a_x^T X(t-1) = u_1(t-1) \quad (21)$$

Consequently, the transformation given by a_x produces the source $u_1(t)$, which has the maximal autocorrelation. The next variates yield $u_i(t)$ that has maximal autocorrelation among all possible linear combination, but they are uncorrelated with the previously $u_{i-1}(t)$. The sources are obtained as $S_i(t) = u_i(t)$. These source signals are uncorrelated with each other, but maximally auto-correlated and in a decrease of autocorrelation index order.

The aim of this section is to remove muscle artifact by using canonical correlation analysis (CCA). According to the visual inspection by experienced experts, the movement-triggered segments are obtained, which contain not only muscle activity but also the activity from the brain. When applying BSS-CCA in the extracted movement-triggered segment, the muscle artifact is supposed to be removed through setting artefactual sources equal to zero. For the reconstructed segment

$$X_{denoised}(t) = MS(t) \quad (22)$$

with M being the mixing matrix with the zero value of muscle artifact sources, and $S(t)$ the

sources calculated by BSSCCA. The investigation in (Goncharova et al., 2003) has identified the common noise-like pattern of EMG contamination that comprises irregular spikes. Thus, a low autocorrelation is expected for muscle artifact, and we assume it is present in the lowest auto-correlated BSSCCA source.

The pre-movement segment is selected as underlying brain signal for comparison, and in the selected EEG signals, we assume that no muscle artifact exists.

5.2 Independent component analysis (ICA)

In the beginning, Independent component analysis (ICA) was proposed for separating source signals from the mixtures by statistical properties, which is widely known as the cocktail-party problem (Hyvriinen & Oja, 2000). With the increasing interest of ICA, there are a variety of practical real-life applications which includes for example biomedical signal analysis and processing. As for EEG signal, it measures the electrical potentials in different locations over the scalp. The brain activity can be regarded as a mixture of the underlying components. Based on the assumption that the source components are statistically independent, the source signals of the brain can be separated from the mixture EEG potentials.

In the ICA model, assuming that we obtain the raw EEG data $X(t)$ in time domain, which is represented as $X(t) = [x_1(t), x_2(t), \dots, x_R(t)]^T (t = 1, \dots, N)$, with N being the number of sample points and R the number of channels. While the underlying independent components are represented by $S(t) = [s_1(t), s_2(t), \dots, s_R(t)]^T$. The mixing model can be written as:

$$X(t) = MS(t) \tag{23}$$

where M is the mixing matrix. The independent components and the mixing matrix cannot

be observed directly, however, both of them are estimated from the mixture $X(t)$ with general assumptions. Apart from the assumption of spatial statistical independence of sources, we also assume that the independent component should follow non-Gaussian distribution. Moreover, the unknown mixing matrix is always assumed to be square. After obtaining the matrix M , its inverse, which is represented as A , can be used to compute the independent component by:

$$S(t) = AX(t) \quad (24)$$

For artifact removal, EEG data recorded from the scalp can be considered as summations of EEG data and artifact, and the contaminating noise can be assumed to be independent of the underlying brain sources. Based on ICA which is also a blind source separation (BSS) problem, this method transforms the input vector into a signal space in which the signals are statistically independent. After the transformation of the EEG signals, non-artifact neural sources should be selected and reconstructed without the artefactual components.

The subjective and time-consuming selection of ICA components is a typical problem for researchers. To reduce the user dependent factor, in this thesis, we have applied an automatic method named Multiple Artifact Rejection Algorithm (MARA) for classification of general artefactual source components. This method is proposed in (Winkler, Haufe, & Tangermann, 2011) and it proves to be an efficient and reliable to detect all classes of artifacts, such as eye and muscle artifacts. Based on six constructed features, MARA incorporates the information from temporal, spectral and spatial domain of the components. This classifier was trained by brain experts based on a large amount of data. It provides an open-source plug-in for a widely-used graphic user interface named EEGLAB (Delorme & Makeig, 2004), in order to automatize the process of hand-labeling independent components. Since ICA is sensitive to slow drifts, band-pass filtering the data can improve the quality of the decomposition. The EEG data are filtered offline before segmentation and artifact removal process, by using an FIR filter in advance. The power spectrum between 2

Hz and 39 Hz is recommended for feature calculation in MARA.

For an automatic classification method, substantial information need to be provided in feature extraction process. Based on the characteristic of independent component, an initial feature set with the collection of 38 features as candidates is constructed, which contains 13 features derived from a component's time series, 9 features from spectrum and 16 from component's pattern. These six features were selected out of 38 features by a feature selection procedure in (Winkler et al., 2011).

- Current density norm

The information of source locations cannot be provided by independent component itself, however, it can be estimated by EEG potentials in ICA scalp map.

- Range within pattern

In a scaly map, the logarithm of the difference between the minimal and the maximal activation is calculated. A high range within pattern always indicates that the spatially located scalp map is generated from muscle artifact or loose electrodes.

- Mean local skewness

This feature is derived from a components time series, and it is obtained by the mean absolute local skewness of time intervals with a duration of 15s, with the purpose of detecting outliers in time domain.

- λ and fit error

The deviation of one component's spectrum from a 1/frequency curve and its shape can be described by two features. For each component, the prototypical curve can be shaped by six points of the log spectrum, including 1) the log power at 2 Hz, 2) the log power at 3 Hz, 3) local minimum point in the band 5 -13 Hz, 4) the point 1 Hz below the third point, 5) local minimum point in the band 33-39 Hz, 6) the point

1Hz below the fifth point. The logarithm of λ and the mean squared error of the approximation of f to the real spectrum in 8 to 15 Hz range are applied as features.

- 8-13 Hz

This feature indicates the average log band power of alpha band from 8 to 13 Hz, with the purpose of detecting the alpha peak in the component of neural origin.

After the automatic classification of artefactual components by MARA, EEGLAB provides the interface to help the experimenters visualize all the independent components and calibrate the components for rejection. Moreover, for each independent components, the scalp map and spectrum are provided for visualization, as well as the probability of being an artifact computed by MARA.

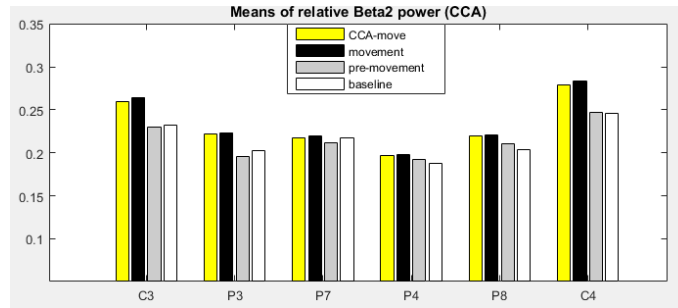
5.3 Experimental results

In this section, we define two consecutive EEG periods to perform the variability tracking, named as reconstructed period and context period, respectively. In reconstructed period, the statistical significance is examined by comparing the parameter difference of reconstructed segments and pre-movement segments. In context period, the parameter difference of pre-movement and baseline segments are compared for statistical analysis.

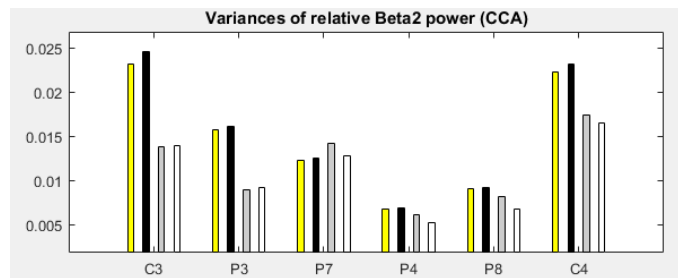
5.3.1 CCA

Relative Beta2 power

Wilcoxon signed rank test shows that there is no significant difference for all six channels between the reconstructed segment after CCA and pre-movement segment. Compared with the result of original data, the difference changes in C4 channel.



(a)



(b)

Figure 5.3: Comparison of means (a) and variances (b) of relative Beta2 power for each channel after applying CCA.

Figure 5.3 gives the mean and variance comparison for all the six channels. As shown, the mean value of the reconstructed segments decreases after applying CCA, and the same trend exists in variance as well.

For all channels, the EEG signal is characterized with relative Beta2 power dominating over anterior areas, as shown in Figure 5.4. Compared with the colored channels identified in Figure 4.9 (Section 4.3.1), significant differences still exist in almost all these colored channels except C4.

Spectral edge frequency (SEF)

After removing artifact by using BSS-CCA algorithm, the statistical differences in SEF medians between pre-movement segments and movement-triggered segments (in test period) are shown in Figure 5.5. This result suggests that there are more channels in central area which change the power distribution in the frequency domain.

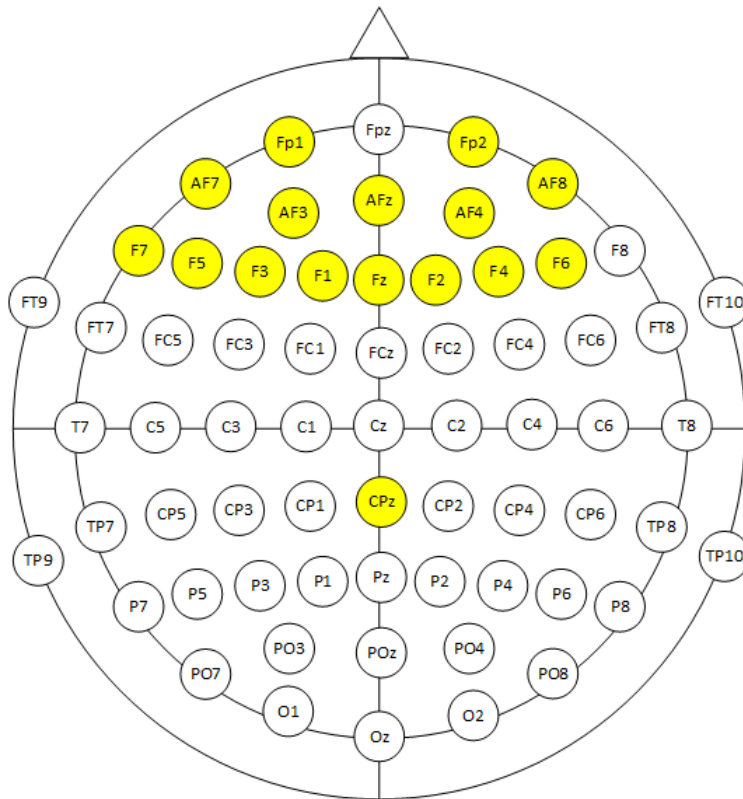
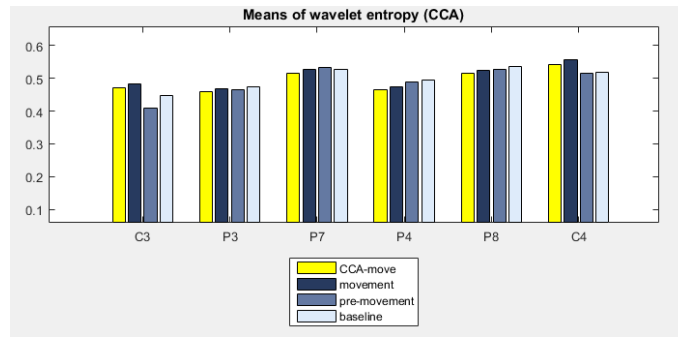
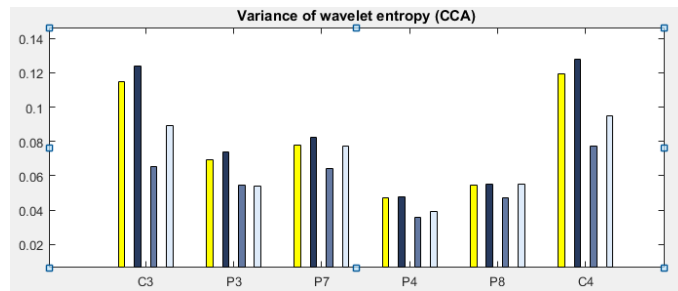


Figure 5.4: Statistical analysis of relative Beta2 power for all channels after applying CCA.



(a)



(b)

Figure 5.6: Comparison of means (a) and variances (b) of wavelet entropy for each channel after applying CCA.

Wavelet entropy

Figure 5.6 shows the mean and variance of wavelet entropy for all six channels, and the comparison in four types of segments. After applying CCA for movement-triggered segments, both the mean and the variance values of WE reduce for all six channels. Statistical analysis illustrates that no significant difference exists between wavelet entropies by Friedman test.

For investigating the transition of wavelet entropy, statistical analysis is applied in relative wavelet entropy for all channels. Figure 5.7 presents the result of the relative wavelet entropy difference when employed on the EEG data for all channels using CCA technique. Compared with the result shown in Figure 4.13 (Section 4.3.2), the degree of similarity between context period and test period changes in more channels after artifact removal.

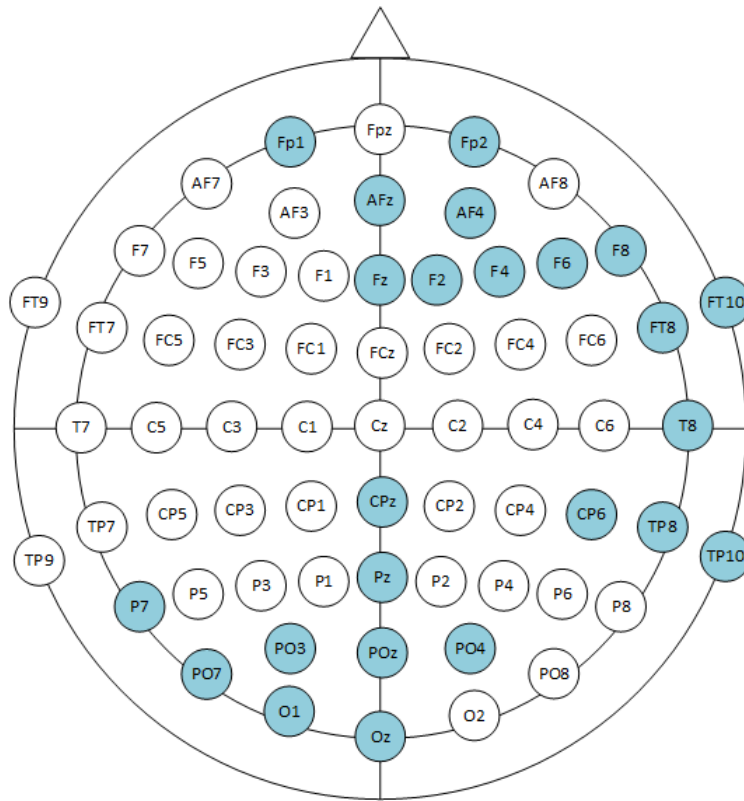
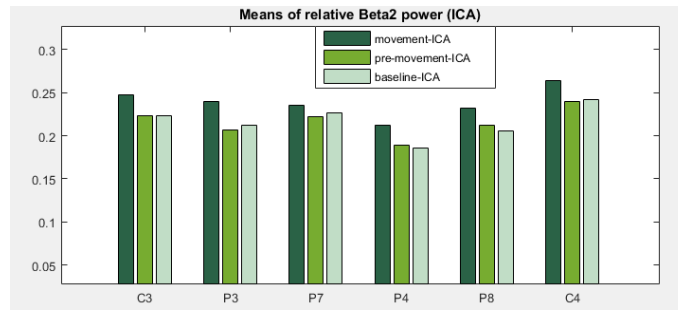
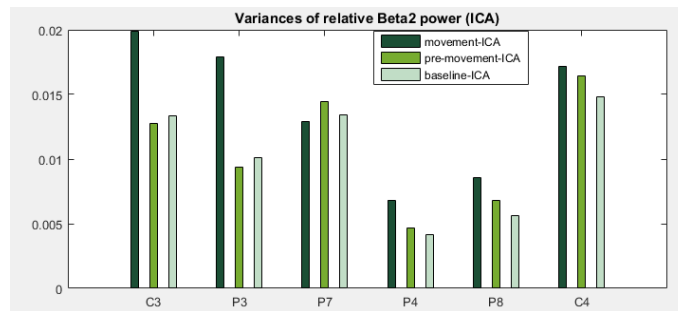


Figure 5.7: Statistical analysis of relative wavelet entropy (RWE) for all channels after applying CCA.



(a)



(b)

Figure 5.8: Comparison of means (a) and variances (b) of relative Beta2 power for each channel after applying ICA.

5.3.2 ICA

After applying ICA method in EEG data, Wilcoxon signed rank test shows that there is significant difference in test period for P3, P4 and P8 channels. From the right-tailed hypothesis test, the median beta2 relative power is greater than the median value before the movement (in P3, P4, P8 and C4 channels).

For all the six channels, Figure 5.8 shows the mean value of relative Beta2 power in three types of segments. Based on the data we obtained from all eight subjects, it can be observed that even though ICA method has applied to the original EEG signals, the mean value in movement-triggered segment is still greater than the other two types of segments. As for the variance of relative Beta2 power, five channels have the highest variances in movement-triggered segment except P7, compared with pre-movement and baseline segment.

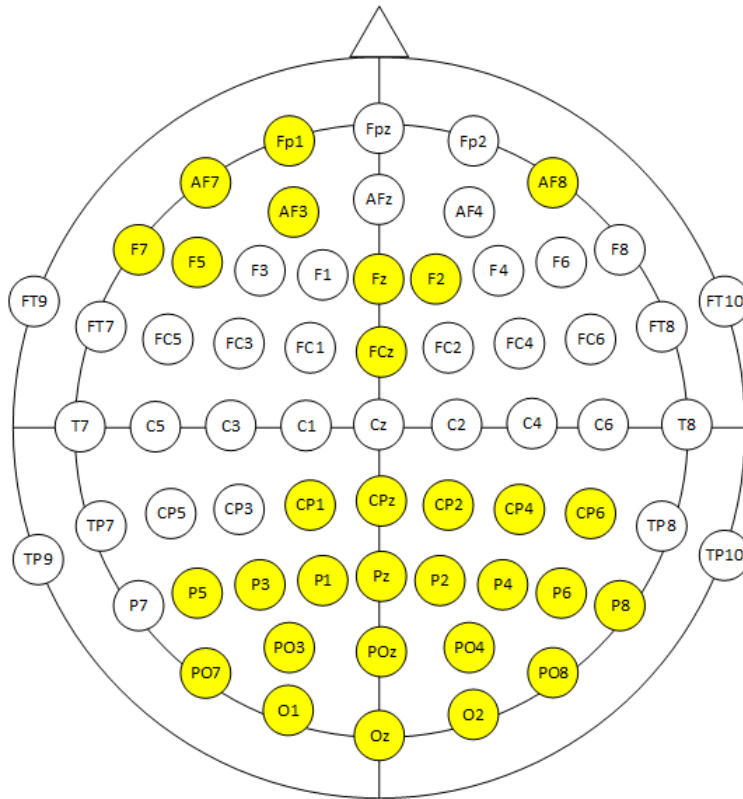
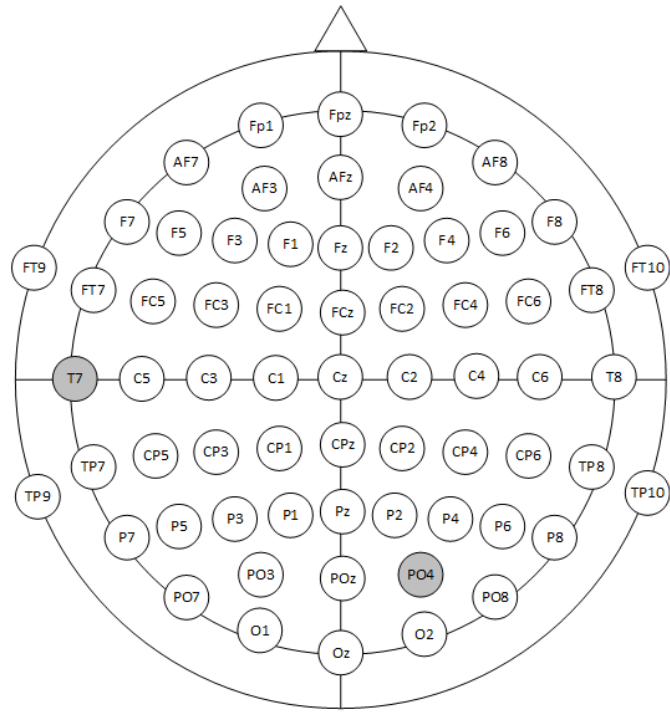


Figure 5.9: Statistical analysis of relative Beta2 power for all channels after applying ICA.

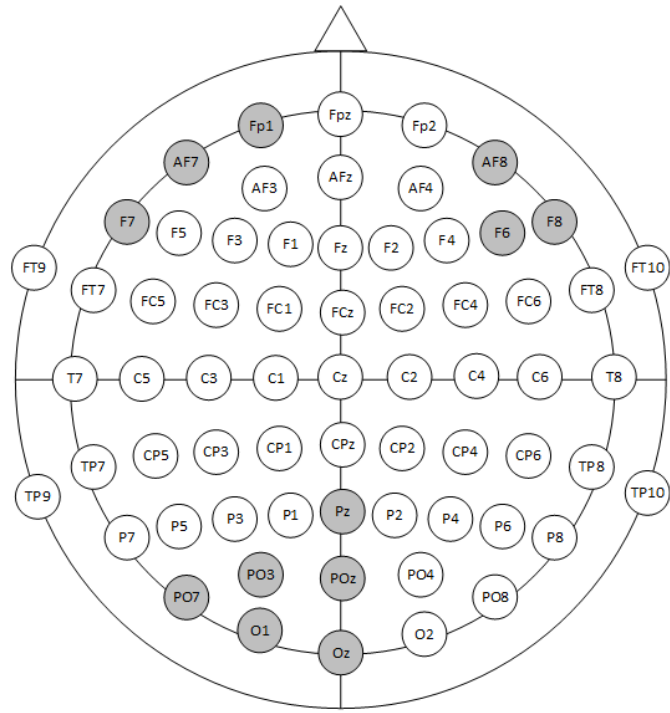
We also applied the statistical analysis for relative Beta2 power on all channels, the result is shown in Figure 5.9.

Spectral edge frequency (SEF)

After applying ICA-MARA, Figure 5.10 shows the statistical result of SEF for all channels in both context period and test period. The significant differences of two channels (T7 and PO4), which exist in SEF medians between pre-movement segments and baseline segments, disappear in test period. While there are many other channels which show the statistical differences.

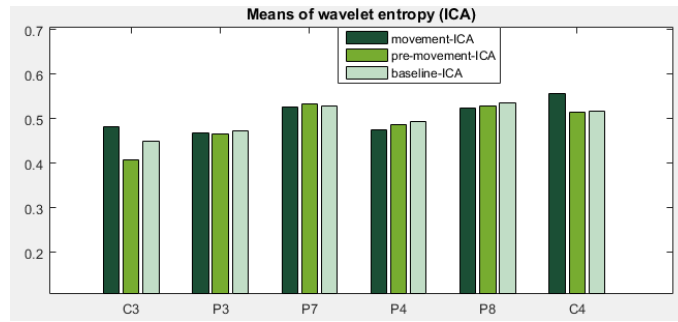


(a)

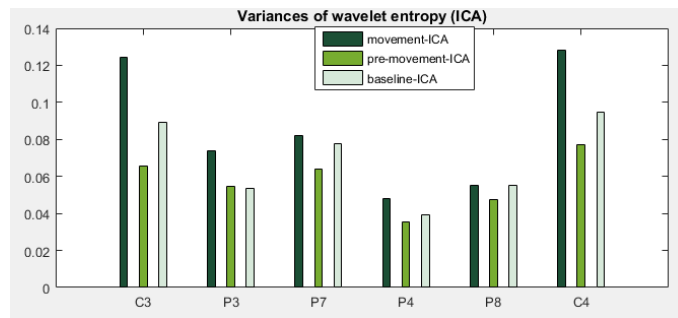


(b)

Figure 5.10: Statistical analysis of spectral edge frequency (SEF) for all channels in context period (a) and test period (b) after applying ICA.



(a)



(b)

Figure 5.11: Comparison of means (a) and variances (b) of wavelet entropy for each channel after applying ICA.

Wavelet entropy

After removing artifact components by using ICA-MARA, the reconstructed signals are applied for feature extraction.

Figure 5.11 illustrates the mean and variance of wavelet entropy after using ICA for all six channels, and the comparison in three types of segments. From the result, we could conclude that when the movement occurs, the variance of WE is significantly larger than the pre-movement and baseline segments. We have also conducted statistical analysis for all channels, and the result illustrates that no significant difference exists in wavelet entropy by Wilcoxon signed rank test.

For further comparison of wavelet entropy, relative wavelet entropy is also applied, in order to measure the degree of similarity in the reconstructed period and context period.

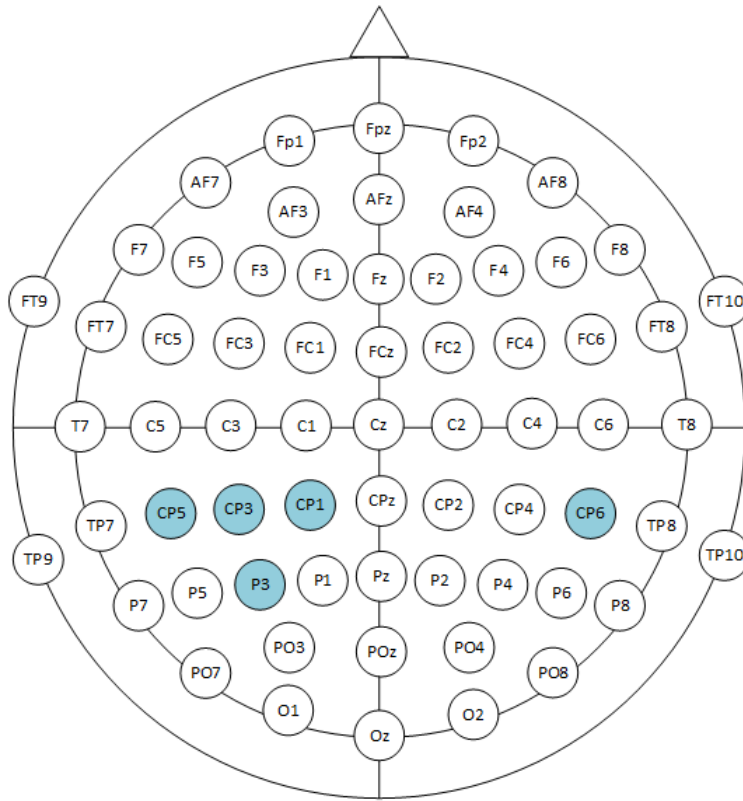


Figure 5.12: Statistical analysis of relative wavelet entropy (RWE) for all channels after applying ICA.

From the result of wavelet entropy we obtained before, the difference of RWE in the reconstructed period and context period is examined by statistical analysis.

Wilcoxon signed rank test shows that there is a significant difference between the RWE in five channels (CP1, CP3, CP5, CP6 and P3) at the 5% significance level. The difference distribution of RWE is shown in Figure 5.12.

5.4 Discussion

In this chapter, we applied two typical blind source separation (BSS) approaches, namely canonical correlation analysis (CCA) and independent component analysis (ICA), to remove the movement artifacts from EEG signals. However, based on the experimental results and comparison study, these two methods have not well performed for removing the movement-triggered artifacts.

After applying CCA method, significant statistical difference of the relative Beta2 power still exist between pre-movement and movement-triggered epochs of all the marked channels (except C4) in frontal lobe of the scalp. While after ICA, the spatial distribution of the marked channels changes. Furthermore, according to the RWE feature which is a way of measuring the degree of similarity, the number of marked channels is reduced. And the marked channels are obtained by comparing the RWE of a context period and the RWE of a test period.

Actually, there exist some limitations with the two typical methods for artifact removal. As for canonical correlation analysis (CCA), it assumes that the autocorrelation of the sources influenced by movements is lower than the autocorrelation of brain sources. However, the problem remaining to be discussed is how many sources need to be rejected.

For ICA method, MARA classifier is trained by experts on large dataset, however, the performance is somehow uncertain in cognitive design process for other movements in which the classifier was not trained. To discriminate artefactual and neuronal source components, the problem of which features are suited is essential to deal with. Therefore, another thing to be argued is the six features used in the classifier construction, which are probably not the overall optimal choice.

Chapter 6

Conclusion and Future Work

6.1 Conclusion

During the course of performing a design task, a variety of movements of the subject can be generated with or without awareness. The main focus in this research is to analyze the design-stimulated movements, which are the voluntary short-time movements accompanied with the cognitive process, rather than the essential and unavoidable body motions that are related to answering question and for giving solutions, named as design-related movements. Based on the video recording, this type of movements is extracted through a predefined guideline proposed in this thesis.

In the present study, a graphic user interface has been developed, and the effects of un-specific body motion have been investigated based on statistical differences between signal features while subjects are working on the cognitive design tasks. Our research results revealed that the relative Beta2 power (20-30Hz) and relative wavelet entropy (RWE) can be applied to differentiate specific physiological brain states under the background brain activities and movement conditions. For the most of channels in the front region of the scalp, a significant decrease in relative Beta2 power is observed in movement-triggered segments. Besides, the statistical analysis result of RWE in some channels indicates that the degree

of similarity changes when movement occurs. Furthermore, two commonly used methods, canonical correlation analysis (CCA) and independent component analysis (ICA), are performed to remove the movement-triggered artifacts, whose performances are evaluated according to the features in both time and frequency domains. The results indicate that these two techniques are insufficient to remove these movement artifacts.

As demonstrated by the experimental results, the significant differences between pre-movement and movement-triggered epochs usually exist in front region of the scalp, which has, in neuro-physiological field, two main sections in the frontal lobe of primates like human: prefrontal cortex that is related to cognitive functions, and caudal cortex which is associated with movement control. The distinction between these two sectors is that the latter lacks granular cells. This agranular frontal cortex can be further divided into several anatomically and functionally distinct areas, each of which represents one independent body movement as reviewed in (Rizzolatti, Luppino, & Matelli, 1998). Recent studies have shown that motor and premotor cortical regions not only control the preparation and execution of voluntary movements, but also are engaged in the high level perceptual and cognitive functions (Rizzolatti & Luppino, 2001) (Mendoza & Merchant, 2014). On the other hand, body movements can affect the thought in problem solving (Thomas & Lleras, 2009).

Since the two artifact removal techniques have not well performed as we expected, the feasibility of eliminating the movement-triggered artifacts should be reconsidered. The definition of artifacts is the potential differences caused by extra-cerebral sources during EEG tracing, more precisely, either by non-neural physiological activities of human or by external technical sources. However, when the body movements have an effect on mental activities, whether the movement-triggered artifacts can still be regarded as non-neural artifacts or not remains to be discussed and explored.

6.2 Future Work

Artifact removal of EEG signal has always been an open and challenging research problem. In the past few decades, a number of approaches have been developed for achieving artifact removal in EEG signals. However, it is still difficult to find out a single best method which is efficient for a wide range of conditions, as it is illustrated in (K. T. Sweeney et al., 2012). Besides classical techniques in signal processing, such as filtering and blind source separation, several algorithms which combine two or more currently available methods have been proposed in recent years. For example, Inuso, Foresta, Mammone, and Morabito (2007) presented a new technique based on the joint use of Wavelet transform and Independent Component Analysis (WICA), and showed that WICA performs very well and allows for minimum information loss. After that, ensemble EMD-ICA (EEMD-ICA) was introduced in (Mijovic, Vos, Gligorijevic, Taelman, & Huffel, 2010), which combines empirical-mode decomposition with independent component analysis. The performance of this method is slightly better than WICA in artifact removal simulations.

For future work, the collection of a bigger database with more subjects would be recommended. Since the sources of movements generated by subjects are usually random for the existing experiments, these body movements of subjects could be divided into several types for a more detailed analysis. In order to obtain the characteristics of movement-triggered artifacts, the applicability of more features, apart from the proposed ones, could be investigated. Moreover, several preliminary experiments for the learning of artifacts could be conducted before cognitive experiments, for the purpose of investigating the individual pattern associated with different types of muscle contractions.

Furthermore, the availability of reference signals should be considered when recording physiological signals. For example, to remove muscle artifact, EMG surface electrodes could be placed at certain positions during design process. Thus, the recorded EMG signals will reflect intervals of specific muscle activation, and obtain the delineation of the

onset and end time of each movement more precisely. Instead of using video recording for manual segmentation, which is really time-consuming, EMG signals can provide additional information and improve the accuracy in time domain. After specifying the epochs of data samples in the prolonged EEG recordings, methods of signal processing and artifact removal can be applied to these epochs where artifacts are most likely present, with the consideration of a low computational cost. At the same time, it is also suggested to include additional electromyographic electrodes as references, especially located over main muscle groups. The collection of EOG signal is also beneficial for the EEG artifact removal process, and it is extremely important for frontal and temporal lobes of brain.

References

- Adeli, H., Zhou, Z., & Dadmehr, N. (2003). Analysis of {EEG} records in an epileptic patient using wavelet transform. *Journal of Neuroscience Methods*, 123(1), 69 - 87. Retrieved from <http://www.sciencedirect.com/science/article/pii/S0165027002003400> doi: [http://dx.doi.org/10.1016/S0165-0270\(02\)00340-0](http://dx.doi.org/10.1016/S0165-0270(02)00340-0)
- Ahmadian, P., Cagnoni, S., & Ascari, L. (2013). How capable is non-invasive eeg data of predicting the next movement? a mini review. *Front Hum Neurosci*, 7. (Ahmadian, Pouya Cagnoni, Stefano Ascari, Luca Front Hum Neurosci. 2013;7:124. doi:10.3389/fnhum.2013.00124.)
- Alexiou, K., Zamenopoulos, T., Johnson, J. H., & Gilbert, S. J. (2009). Exploring the neurological basis of design cognition using brain imaging: some preliminary results. *Design Studies*, 30(6), 623-647. Retrieved from <http://www.sciencedirect.com/science/article/pii/S0142694X09000313>
- Al-Fahoum, A. S., & Al-Fraihat, A. A. (2014). Methods of eeg signal features extraction using linear analysis in frequency and time-frequency domains. *ISRN Neuroscience*, 2014, 730218. Retrieved from <http://www.ncbi.nlm.nih.gov/pmc/articles/PMC4045570/>
- Anderer, P., Roberts, S., Schlgl, A., Gruber, G., Klsch, G., Herrmann, W., ... Saletu, B. (1999). Artifact processing in computerized analysis of sleep eeg a review. *Neuropsychobiology*, 40(3), 150-157. Retrieved from <http://www.karger.com/>

[DOI/10.1159/000026613](https://doi.org/10.1159/000026613)

- Berka, C., Levendowski, D. J., Lumicao, M. N., Yau, A., Davis, G., Zivkovic, V. T., ... Craven, P. L. (2007). Eeg correlates of task engagement and mental workload in vigilance, learning, and memory tasks. *Aviation, Space, and Environmental Medicine*, 78(5), B231-B244.
- Berka, C., Levendowski, D. J., Westbrook, P., Davis, G., Lumicao, M. N., Olmstead, R. E., ... Ramsey, C. K. (2005). Eeg quantification of alertness: methods for early identification of individuals most susceptible to sleep deprivation. , 5797, 78-89. Retrieved from <http://dx.doi.org/10.1117/12.597503>
- Brittenham, D. (1974). Recognition and reduction of physiological artifacts. *American Journal of EEG Technology*, 14(2-3), 158-165.
- Carskadon, M. A., & Rechtschaffen, A. (2000). Monitoring and staging human sleep. *Principles and practice of sleep medicine*, 3, 1197-1215.
- Clercq, W. D., Vergult, A., Vanrumste, B., Paesschen, W. V., & Huffel, S. V. (2006). Canonical correlation analysis applied to remove muscle artifacts from the electroencephalogram. *IEEE Transactions on Biomedical Engineering*, 53(12), 2583-2587.
- Cohen, B. H., Davidson, R. J., Senulis, J. A., Saron, C. D., & Weisman, D. R. (1992). Muscle tension patterns during auditory attention. *Biological Psychology*, 33(23), 133-156. Retrieved from <http://www.sciencedirect.com/science/article/pii/030105119290028S>
- Committee, E. P. N. (1994). Guideline thirteen: guidelines for standard electrode position nomenclature. *J Clin Neurophysiol*, 11, 111-3.
- Conforto, S., D'Alessio, T., & Pignatelli, S. (1999). Optimal rejection of movement artefacts from myoelectric signals by means of a wavelet filtering procedure. *Journal of Electromyography and Kinesiology*, 9(1), 47 - 57. Retrieved from <http://www.sciencedirect.com/science/article/>

[pii/S1050641198000236](http://dx.doi.org/10.1016/S1050-6411(98)00023-6) doi: [http://dx.doi.org/10.1016/S1050-6411\(98\)00023-6](http://dx.doi.org/10.1016/S1050-6411(98)00023-6)

- Croft, R. J., & Barry, R. J. (2000). Removal of ocular artifact from the eeg: a review. *Neurophysiologie Clinique/Clinical Neurophysiology*, 30(1), 5-19. doi: [http://dx.doi.org/10.1016/S0987-7053\(00\)00055-1](http://dx.doi.org/10.1016/S0987-7053(00)00055-1)
- Croft, R. J., & Barry, R. J. (2002). Issues relating to the subtraction phase in eeg artefact correction of the eeg. *International Journal of Psychophysiology*, 44(3), 187-195. Retrieved from <http://www.sciencedirect.com/science/article/pii/S016787600100201X>
- Deecke, L., Scheid, P., & Kornhuber, H. H. (1969). Distribution of readiness potential, pre-movement positivity, and motor potential of the human cerebral cortex preceding voluntary finger movements. *Experimental Brain Research*, 7(2), 158–168. Retrieved from <http://dx.doi.org/10.1007/BF00235441> doi: 10.1007/BF00235441
- Delorme, A., & Makeig, S. (2004). Eeglab: an open source toolbox for analysis of single-trial {EEG} dynamics including independent component analysis. *Journal of Neuroscience Methods*, 134(1), 9 - 21. Retrieved from [//www.sciencedirect.com/science/article/pii/S0165027003003479](http://www.sciencedirect.com/science/article/pii/S0165027003003479) doi: <http://dx.doi.org/10.1016/j.jneumeth.2003.10.009>
- Farina, D., do Nascimento, O. F., Lucas, M.-F., & Doncarli, C. (2007). Optimization of wavelets for classification of movement-related cortical potentials generated by variation of force-related parameters. *Journal of Neuroscience Methods*, 162(12), 357 - 363. Retrieved from <http://www.sciencedirect.com/science/article/pii/S0165027007000362> doi: <http://dx.doi.org/10.1016/j.jneumeth.2007.01.011>
- Fatourechi, M., Bashashati, A., Ward, R. K., & Birch, G. E. (2007). Emg and eeg

- artifacts in brain computer interface systems: A survey. *Clinical Neurophysiology*, 118(3), 480-494. Retrieved from <http://www.sciencedirect.com/science/article/pii/S1388245706015124>
- Gazzaniga, M. S. (1989). Organization of the human brain. *Science*, 245(4921), 947-952.
- Gevins, A., & Smith, M. E. (2003). Neurophysiological measures of cognitive workload during human-computer interaction. *Theoretical Issues in Ergonomics Science*, 4(1-2), 113-131. Retrieved from <http://dx.doi.org/10.1080/14639220210159717>
- Gevins, A., Smith, M. E., Leong, H., McEvoy, L., Whitfield, S., Du, R., & Rush, G. (1998). Monitoring working memory load during computer-based tasks with eeg pattern recognition methods. *Human Factors: The Journal of the Human Factors and Ergonomics Society*, 40(1), 79-91.
- Goljahani, A., D'Avanzo, C., Schiff, S., Amodio, P., Bisiacchi, P., & Sparacino, G. (2012). A novel method for the determination of the eeg individual alpha frequency. *NeuroImage*, 60(1), 774-786. Retrieved from <http://www.sciencedirect.com/science/article/pii/S105381191101398X>
- Goncharova, I., McFarland, D., Vaughan, T., & Wolpaw, J. (2003). {EMG} contamination of eeg: spectral and topographical characteristics. *Clinical Neurophysiology*, 114(9), 1580 - 1593. Retrieved from <http://www.sciencedirect.com/science/article/pii/S1388245703000932> doi: [http://dx.doi.org/10.1016/S1388-2457\(03\)00093-2](http://dx.doi.org/10.1016/S1388-2457(03)00093-2)
- Guo, L., Rivero, D., Seoane, J. A., & Pazos, A. (2009). Classification of eeg signals using relative wavelet energy and artificial neural networks. In *Proceedings of the first acm/sigevo summit on genetic and evolutionary computation* (pp. 177-184). New York, NY, USA: ACM. Retrieved from <http://doi.acm.org/10.1145/1543834.1543860> doi: 10.1145/1543834.1543860

- Howells, F. M., Stein, D. J., & Russell, V. A. (2010). Perceived mental effort correlates with changes in tonic arousal during attentional tasks. *Behavioral and Brain Functions*, 6(1), 39. Retrieved from <http://dx.doi.org/10.1186/1744-9081-6-39>
- Huigen, E., Peper, A., & Grimbergen, C. A. (2002). Investigation into the origin of the noise of surface electrodes. *Medical and Biological Engineering and Computing*, 40(3), 332-338. Retrieved from <http://dx.doi.org/10.1007/BF02344216>
- Hyvriinen, A., & Oja, E. (2000). Independent component analysis: algorithms and applications. *Neural Networks*, 13(45), 411 - 430. Retrieved from <http://www.sciencedirect.com/science/article/pii/S0893608000000265> doi: [http://dx.doi.org/10.1016/S0893-6080\(00\)00026-5](http://dx.doi.org/10.1016/S0893-6080(00)00026-5)
- Inuso, G., Foresta, F. L., Mammone, N., & Morabito, F. C. (2007, Aug). Wavelet-ica methodology for efficient artifact removal from electroencephalographic recordings. In *2007 international joint conference on neural networks* (p. 1524-1529). doi: 10.1109/IJCNN.2007.4371184
- Jasper, H. H. (1958). The ten twenty electrode system of the international federation. *Electroencephalography and Clinical Neurophysiology*, 10, 371-375. Retrieved from <http://ci.nii.ac.jp/naid/10020218106/en/>
- Jung, T.-P., Makeig, S., Humphries, C., Lee, T.-W., McKeown, M. J., Iragui, V., & Sejnowski, T. J. (2000). Removing electroencephalographic artifacts by blind source separation. *Psychophysiology*, 37(2), 163-178. Retrieved from <http://dx.doi.org/10.1111/1469-8986.3720163> doi: 10.1111/1469-8986.3720163
- Klass, D. W. (1995). The continuing challenge of artifacts in the eeg. *American Journal of EEG Technology*, 35(4), 239-269. Retrieved from <http://www.tandfonline.com/doi/abs/10.1080/00029238.1995.11080524>
- Kline, J. E., Huang, H. J., Snyder, K. L., & Ferris, D. P. (2015). Isolating gait-related

- movement artifacts in electroencephalography during human walking. *Journal of neural engineering*, 12(4), 046022-046022. (26083595[pmid] J Neural Eng)
- Kornhuber, H. H., & Deecke, L. (1965). Hirnpotentialänderungen bei willkürbewegungen und passiven bewegungen des menschen: Bereitschaftspotential und reafferente potentiale. *Pflüger's Archiv für die gesamte Physiologie des Menschen und der Tiere*, 284(1), 1–17. Retrieved from <http://dx.doi.org/10.1007/BF00412364> doi: 10.1007/BF00412364
- Kumar, Y., Dewal, M. L., & Anand, R. S. (2012). Relative wavelet energy and wavelet entropy based epileptic brain signals classification. *Biomedical Engineering Letters*, 2(3), 147–157. Retrieved from <http://dx.doi.org/10.1007/s13534-012-0066-7> doi: 10.1007/s13534-012-0066-7
- Luck, S. J. (2005). Ten simple rules for designing erp experiments. *Event-related potentials: A methods handbook*, 262083337.
- Mallat, S. G. (1989). A theory for multiresolution signal decomposition: the wavelet representation. *IEEE Transactions on Pattern Analysis and Machine Intelligence*, 11(7), 674-693.
- McFarland, D. J., Sarnacki, W. A., Vaughan, T. M., & Wolpaw, J. R. (2005). Brain-computer interface (bci) operation: signal and noise during early training sessions. *Clinical Neurophysiology*, 116(1), 56-62. Retrieved from <http://www.sciencedirect.com/science/article/pii/S1388245704002664>
- McGrogan, N., et al. (1999). Neural network detection of epileptic seizures in the electroencephalogram.
- Mendoza, G., & Merchant, H. (2014). Motor system evolution and the emergence of high cognitive functions. *Progress in Neurobiology*, 122, 73 - 93. Retrieved from <http://www.sciencedirect.com/science/article/>

[pii/S0301008214000999](https://doi.org/10.1016/j.pneurobio.2014.09.001) doi: <http://dx.doi.org/10.1016/j.pneurobio.2014.09.001>

- Mijovic, B., Vos, M. D., Gligorijevic, I., Taelman, J., & Huffel, S. V. (2010, Sept). Source separation from single-channel recordings by combining empirical-mode decomposition and independent component analysis. *IEEE Transactions on Biomedical Engineering*, *57*(9), 2188-2196. doi: 10.1109/TBME.2010.2051440
- Mulert, C., Menzinger, E., Leicht, G., Pogarell, O., & Hegerl, U. (2005). Evidence for a close relationship between conscious effort and anterior cingulate cortex activity. *International Journal of Psychophysiology*, *56*(1), 65-80.
- Nguyen, T. A., & Zeng, Y. (2012). Clustering designers mental activities based on eeg power. *Tools and methods of competitive engineering, Karlsruhe, Germany*.
- Nguyen, T. A., & Zeng, Y. (2014). A physiological study of relationship between designers mental effort and mental stress during conceptual design. *Computer-Aided Design*, *54*, 3-18. Retrieved from <http://www.sciencedirect.com/science/article/pii/S0010448513002005>
- Nguyen, T. A., & Zeng, Y. (2016). Effects of stress and effort on self-rated reports in experimental study of design activities. *Journal of Intelligent Manufacturing*, 1-14. Retrieved from <http://dx.doi.org/10.1007/s10845-016-1196-z>
- Niedermeyer, E., & da Silva, F. L. (2005). *Electroencephalography: basic principles, clinical applications, and related fields*. Lippincott Williams and Wilkins.
- Regan, S. O., Faul, S., & Marnane, W. (2010). Automatic detection of eeg artefacts arising from head movements. In *2010 annual international conference of the ieee engineering in medicine and biology* (p. 6353-6356).
- Reis, P. M. R., Hebenstreit, F., Gabsteiger, F., von Tscharnner, V., & Lochmann, M. (2014). Methodological aspects of eeg and body dynamics measurements during motion.

- Front Hum Neurosci*, 8. (Reis, Pedro M R Hebenstreit, Felix Gabsteiger, Florian von Tscharnher, Vinzenz Lochmann, Matthias Front Hum Neurosci. 2014;8:156. doi:10.3389/fnhum.2014.00156.)
- Ribas, G. C. (2010). The cerebral sulci and gyri. *Neurosurgical focus*, 28(2), E2.
- Rizzolatti, G., & Luppino, G. (2001). The cortical motor system. *Neuron*, 31(6), 889 - 901. Retrieved from [//www.sciencedirect.com/science/article/pii/S0896627301004238](http://www.sciencedirect.com/science/article/pii/S0896627301004238) doi: [http://dx.doi.org/10.1016/S0896-6273\(01\)00423-8](http://dx.doi.org/10.1016/S0896-6273(01)00423-8)
- Rizzolatti, G., Luppino, G., & Matelli, M. (1998). The organization of the cortical motor system: new concepts. *Electroencephalography and Clinical Neurophysiology*, 106(4), 283 - 296. Retrieved from [//www.sciencedirect.com/science/article/pii/S0013469498000224](http://www.sciencedirect.com/science/article/pii/S0013469498000224) doi: [http://dx.doi.org/10.1016/S0013-4694\(98\)00022-4](http://dx.doi.org/10.1016/S0013-4694(98)00022-4)
- Rosso, O. A., Blanco, S., & Figliola, A. (2004). Characterization of the dynamical evolution of electroencephalogram time series. In O. Descalzi, J. Martínez, & E. Tirapegui (Eds.), *Instabilities and nonequilibrium structures vii & viii* (pp. 333–338). Dordrecht: Springer Netherlands. Retrieved from http://dx.doi.org/10.1007/978-1-4020-2149-7_24 doi: 10.1007/978-1-4020-2149-7_24
- Rosso, O. A., Blanco, S., Yordanova, J., Kolev, V., Figliola, A., Schrmann, M., & Baar, E. (2001). Wavelet entropy: a new tool for analysis of short duration brain electrical signals. *Journal of Neuroscience Methods*, 105(1), 65-75.
- Schacter, D. L. (1977). Eeg theta waves and psychological phenomena: A review and analysis. *Biological Psychology*, 5(1), 47-82. Retrieved from <http://www.sciencedirect.com/science/article/pii/030105117790028X>
- Schwender, D., Dauderer, M., Mulzer, S., Klasing, S., Finsterer, U., & Peter, K. (1996).

- Spectral edge frequency of the electroencephalogram to monitor” depth” of anaesthesia with isoflurane or propofol. *British journal of anaesthesia*, 77(2), 179-184.
- Shibasaki, H., & Hallett, M. (2006). What is the bereitschaftspotential? *Clinical Neurophysiology*, 117(11), 2341 - 2356. Retrieved from [//www.sciencedirect.com/science/article/pii/S138824570600229X](http://www.sciencedirect.com/science/article/pii/S138824570600229X) doi: <http://dx.doi.org/10.1016/j.clinph.2006.04.025>
- Solomon Jr, O. M. (1991). *Psd computations using welch’s method.[power spectral density (psd)]* (Tech. Rep.). Sandia National Labs., Albuquerque, NM (United States).
- Sornmo, L., & Laguna, P. (2005). Chapter 3 - eeg signal processing. In *Bioelectrical signal processing in cardiac and neurological applications* (p. 55-179). Burlington: Academic Press. Retrieved from <http://www.sciencedirect.com/science/article/pii/B9780124375529500039>
- Sweeney, K., McLoone, S., & Ward, T. (2010). A simple bio-signals quality measure for in-home monitoring.
- Sweeney, K. T., Ward, T. E., & McLoone, S. F. (2012, May). Artifact removal in physiological signals: Practices and possibilities. *IEEE Transactions on Information Technology in Biomedicine*, 16(3), 488-500. doi: 10.1109/TITB.2012.2188536
- Tang, Y., & Zeng, Y. (2009). Quantifying designers mental stress in the conceptual design process using kinesics study. In *Ds 58-9: Proceedings of iced 09, the 17th international conference on engineering design, vol. 9, human behavior in design, palo alto, ca, usa, 24.-27.08. 2009*.
- Teplan, M. (2002). Fundamentals of eeg measurement. *Measurement science review*, 2(2), 1-11.
- Thomas, L. E., & Lleras, A. (2009). Swinging into thought: Directed movement guides insight in problem solving. *Psychonomic Bulletin & Review*, 16(4), 719–723. Retrieved from <http://dx.doi.org/10.3758/PBR.16.4.719> doi:

10.3758/PBR.16.4.719

- Van de Velde, M., van Erp, G., & Cluitmans, P. J. M. (1998). Detection of muscle artefact in the normal human awake eeg. *Electroencephalography and Clinical Neurophysiology*, *107*(2), 149-158. Retrieved from <http://www.sciencedirect.com/science/article/pii/S0013469498000522>
- Walter, W. (1953). The living brain.
- Welch, P. D. (1967). The use of fast fourier transform for the estimation of power spectra: A method based on time averaging over short, modied periodograms. *IEEE Transactions on audio and electroacoustics*, *15*(2), 70-73.
- Winkler, I., Haufe, S., & Tangermann, M. (2011). Automatic classification of artifactual ica-components for artifact removal in eeg signals. *Behavioral and Brain Functions*, *7*(1), 1-15. Retrieved from <http://dx.doi.org/10.1186/1744-9081-7-30>
- Wolpaw, J. R., & McFarland, D. J. (2004). Control of a two-dimensional movement signal by a noninvasive brain-computer interface in humans. *Proceedings of the National Academy of Sciences of the United States of America*, *101*(51), 17849-17854. Retrieved from <http://www.ncbi.nlm.nih.gov/pmc/articles/PMC535103/>
- Woodman, G. F. (2010). A brief introduction to the use of event-related potentials (erps) in studies of perception and attention. *Attention, perception and psychophysics*, *72*(8), 10.3758/APP.72.8.2031. Retrieved from <http://www.ncbi.nlm.nih.gov/pmc/articles/PMC3816929>